Palaeogeography, Palaeoclimatology, Palaeoecology 422 (2015) 65–84

Contents lists available at ScienceDirect

Palaeogeography, Palaeoclimatology, Palaeoecology

journal homepage: www.elsevier.com/locate/palaeo

Repeated advance and retreat of the East Antarctic Ice Sheet on the continental shelf during the early Pliocene warm period

B.T.I. Reinardy [a,*], C. Escutia [a], M. Iwai [b], F.J. Jimenez-Espejo [c], C. Cook [d,1], T. van de Flierdt [d], H. Brinkhuis [e]

[a] Instituto Andaluz de Ciencias de la Tierra (CSIC), Avenida de las Palmeras 4, 18100 Armilla, Granada, Spain
[b] Department of Natural Science, Kochi University, 2-5-1 Akebono-cho, Kochi 780-8520, Japan
[c] Department of Biogeochemistry, Japan Agency for Marine-Earth Science and Technology (JAMSTEC), Yokosuka 237-0061, Japan
[d] Department of Earth Science and Engineering, Imperial College London, South Kensington Campus, London SW7 2AZ, United Kingdom
[e] Institute of Environmental Biology, Faculty of Science, Utrecht University, Budapestlaan 4, 3584 CD Utrecht, The Netherlands

ARTICLE INFO

Article history:
Received 3 June 2014
Received in revised form 19 December 2014
Accepted 8 January 2015
Available online 14 January 2015

Keywords:
Grounding line
East Antarctic Ice Sheet
Micromorphology
Pliocene
Wilkes Subglacial Basin

ABSTRACT

Diatom analysis of a sediment core recovered at IODP Site U1358 on the continental shelf off the Adélie Coast indicated that the lower section of the core contained an assemblage dating back to the *Thalassiosira innura* Zone of the lower Pliocene that ranges from 4.2 to 5.12 Ma. Based on lithological descriptions at both a macro- and micro-scale of this early Pliocene part of the core, four facies were interpreted from the diamictons representing the progressive advance and retreat of the grounding line over the site. Facies 1a and 1b contain a distinct directional signal from the orientation of the a-axis of clasts with several phases of fabric development along with both brittle and ductile deformation features that are common in sediments that have been subglacially deformed. Facies 1c and 1d are finely laminated and were deposited in open marine conditions. The four facies within the depositional model provide for the first time direct evidence for ice advancing across the shelf adjacent to the Wilkes Subglacial Basin on at least four occasions separated by three periods of open marine conditions indicating retreat of grounded ice inland of the site during a warmer than present early Pliocene. The times of open marine conditions are correlated with previous findings from the neighbouring rise sites that also indicated an oscillating ice margin. This has significant implications because firstly it suggests a dynamic East Antarctic Ice Sheet (EAIS) that is probably far more sensitive to climatic and oceanic forcing even during relatively short time periods than had previously been thought. Secondly it suggests that proxies used to interpret the advance and retreat of the grounding line from the rise can be linked with direct evidence of grounding line migration from the shelf. It also has important implications for the future behaviour and sensitivity of the EAIS under present continuing warming conditions. Together with results from the rise, this paper provides a crucial ice extent target for a new ice sheet model of this region during the Pliocene.

1. Introduction

Polar ice and the expansion and retreat of ice sheets are an important component of the modern climate system, affecting global sea level, ocean circulation, heat transport, marine productivity and planetary albedo among others. With the current rise of atmospheric greenhouse gas concentrations and rapidly increasing global temperatures (IPCC, 2013), studies of polar climates, ice sheet dynamics and (in-)stability are prominent on the research agenda. IPCC (2013) forecasts rising levels of atmospheric CO_2 between 550 and 950 ppm and possible >4 °C warming by 2100 which have not been experienced on our planet since the early to middle Pliocene at ~4.2 to 3.0 Ma (Pagani et al., 2010), with the higher temperature estimates possibly not having been experienced since about 10 to 15 Ma ago. During the early to mid Pliocene, sea level estimates of 22 m above present (Miller et al., 2012) indicate the collapse of not only the Greenland Ice Sheet (7 m sea level equivalent — SLE) and the West Antarctic Ice Sheet (WAIS) (5 m SLE) but also sectors of the EAIS.

While recent satellite observations reveal that the Greenland Ice Sheet and WAIS are losing mass in response to climatic warming, the response of the EAIS has been more variable with increased mass loss through speed up and thinning of outlet glaciers compensated by increased surface accumulation (Pritchard et al., 2009; Shepherd et al., 2012). The EAIS vulnerability to warmer-than-present temperatures may be particularly significant in areas where the EAIS is grounded below sea level and also where the base of the ice sheet is in contact with the Southern Ocean, such as the Wilkes Subglacial Basin. This vulnerability can be studied using the geological record from intervals

* Corresponding author at: Department of Earth Science, University of Bergen, Allegaten 41, N-5007 Bergen, Norway. Tel.: +47 55588112.
E-mail address: Benedict.Reinardy@geo.uib.no (B.T.I. Reinardy).
[1] Present address: Department of Geological Sciences, Williamson Hall, University of Florida, Gainesville, FL 32611-2120, USA.

http://dx.doi.org/10.1016/j.palaeo.2015.01.009
0031-0182/

with similar environmental conditions to those predicted for the near future. Studies from the continental rise and slope as well as the deep ocean have used multiple proxies such as sediment facies and grain size, IRD concentrations, siliceous microfossils, biogenic opal, geochemical composition and clay mineralogy to interpret ice sheet dynamics in response to varying palaeoenvironmental conditions (e.g. Bart et al., 2007; Escutia et al., 2009; Williams et al., 2010; Passchier, 2011; Cook et al., 2013). During the early Pliocene (3.6 to 5.3 Ma), Southern Ocean sea surface temperatures (SST) north of Prydz Bay reached over 5 °C warmer than present (Bohaty and Harwood, 1998; Whitehead and Bohaty, 2003; Escutia et al., 2009), and winter sea ice was reduced up to 78% compared to present day (Whitehead et al., 2005). Although these data are relevant for palaeoenvironmental conditions linked to the advance and retreats of the ice sheet during glacial and interglacial cycles respectively, they cannot trace the migration of the grounding line and thus cannot constrain the lateral extent of grounded ice. This constraint is critical if estimations are to be made regarding sea level change. The location of the grounding line in turn can only be determined from continental shelf records. For example, the ANDRILL (AND-1B) core drilled below the Ross Ice Shelf allowed Naish et al. (2009) and Pollard and DeConto (2009) to model total collapse of WAIS during warm early Pliocene times while at other times during the Pliocene the ice cover in the Ross Sea was greater than the current modern extent.

The aim of this paper is to provide direct evidence of either open marine conditions or the presence of grounded ice offshore from the Wilkes Subglacial Basin during the early Pliocene warm interval (i.e., 3.6 to 5.3 Ma) and thus test the interpretations made from other rise and deep ocean sites that assert a dynamic EAIS with several advances and retreats of the grounding line across the shelf (Bart, 2001; Escutia et al., 2005, 2009, 2011; Williams et al., 2010; Cook et al., 2013). Thus, the opportunity is provided to link the fluctuations and glacial–interglacial cyclicity reported from both the rise and deep ocean sediments in addition to those predicted by ice sheet models (Mengel and Levermann, 2014), with direct evidence of grounding line migration.

1.1. Ice sheet fluctuations during the early Pliocene

Some of the earliest models of the Antarctic ice sheets suggested that warmer than present climatic conditions would lead to an increase in ice volume (Oerlemans, 1982; Huybrechts, 1994) and more recently studies indicate that since their inception, the Antarctic ice sheets have been very dynamic, waxing and waning (DeConto and Pollard, 2003). This includes the margins of the EAIS, particularly those parts grounded below sea level (i.e., in the Wilkes Subglacial Basin) and the marine-based WAIS (Pollard and DeConto, 2009; Mengel and Levermann, 2014). Some of these models also indicated significant variations in ice sheet volume during the Pliocene (Hill et al., 2007; Dolan et al., 2011; Haywood et al., 2012). Seismic stratigraphy from the Antarctic margin has also identified major erosional events linked to glacial cycles (e.g. Eittreim et al., 1995; Escutia et al., 1997, 2005; Barker et al., 1999; Bart et al., 1999; Bart, 2001; De Santis et al., 2003; Rebesco et al., 2006; Cooper et al., 2009).

Diatomite units recovered in the early Pliocene section of the AND-1B core point to persistent open marine conditions with grounded ice inland of the site (McKay et al., 2009; Naish et al., 2009). It is during these periods that models also show the collapse of WAIS (Pollard and DeConto, 2009). It is unclear whether similar advance and retreat phases occurred on the shelf of other regions bordering the EAIS. However, Cook et al. (2013) have used geochemical provenance of detrital material in sediments from the continental rise to suggest active erosion of continental bedrock from within the Wilkes Subglacial Basin and retreat of EAIS in this area several hundred kilometres inland during early Pliocene times. In addition, Williams et al. (2010) show that the provenance of ice-rafted detritus also on the continental rise of East Antarctica at 3.5 Ma and 4.6 Ma saw significant increases in iceberg production into the Southern Ocean from along the Wilkes Land and Adélie Land margins.

Direct evidence of grounded ice migration can only be derived from shelf sites. Micromorphological and fabric analyses of sediment cores from the shelf provide a key piece of evidence when trying to differentiate between subglacial and glacimarine sediments because they are deposited by different processes and thus have different micro-scale sedimentary signatures (Reinardy et al., 2011a,b).

2. Drilling site and regional setting

Integrated Ocean Drilling Program (IODP) Expedition 318 drilled a transect of sites across the Wilkes Land margin of Antarctica to provide a long-term record of the sedimentary archives of Cenozoic Antarctic glaciation and its relationship with global climatic and oceanographic change. Drilling was undertaken to constrain the age, nature, and palaeoenvironment of the previously only seismically inferred glacial sequences (Escutia et al., 2005, 2011). Site U1358 is situated on the outer continental shelf off the Adélie Coast at the mouth of the north western end of the George V Basin at 499 mbsl and receives drainage from the EAIS through the Wilkes Subglacial Basin (Fig. 1). The location of the site is significant because the EAIS in this sector is grounded below sea level and it has the potential to become unstable and could have contributed to sea level rise during past times of warmth (Escutia et al., 2005, 2011; Cook et al., 2013; Mengel and Levermann, 2014).

Site U1358 and the regional stratigraphy based on seismic data are described in detail in Escutia et al. (2005, 2011) and are only briefly mentioned here. It is important to note that glacimarine and subglacial deposits cannot always be differentiated from seismic data because both can have very similar acoustic characteristics and the interpretation of glacial stratigraphy using seismic data alone can be problematic (Stoker et al., 1992). Hole 1358B penetrated 35.6 mbsf into steep foresets above unconformity WL-U8 which has previously been suggested to be deposited in front of grounded ice sheets that extended intermittently onto the outer shelf (Eittreim et al., 1995; Escutia et al., 2005; Cooper et al., 2009). Because the hole had to be terminated before weight-on-bit could be applied, the total cored interval for 1358B was 35.6 m but the total core recovery was only 8 m of diamicton.

3. Methods

Cores from Hole U1358B were recovered using a rotary core barrel system. This study focuses on the two lower cores below 17.3 mbsf. These are core 3R consisting of 3 sections, 3R-1 to 3 and core 4R also consisting of 3 sections, 4R-1 and 2 and 4R-CC (Fig. 2). 3R and 4R have been assigned a Pliocene age by Escutia et al. (2011) and Orejola et al. (2014). The diatom assemblage was used to refine this age model (see discussion below). For dating and micromorphology, it is important to note that cores 3R and 4R were not significantly disturbed by the coring process (Escutia et al., 2011).

3.1. Micromorphological analysis and fabric data

Both macro- and micro-scale descriptions and interpretations were carried out on cores 3R and 4R. Micromorphology is a particularly effective technique used to interpret depositional environments from sediments that appear massive at a macro-scale and where there are only limited exposures as is the case with sediment cores. Micromorphology has previously been used to provide evidence of grounded ice at Cape Roberts (van der Meer and Hiemstra, 1998; Hiemstra, 1999; van der Meer, 2000). The technique has also been used on Antarctic sediments to indicate basal thermal regime (Baroni and Fasano, 2006), deformation processes (Evans et al., 2005; Ó Cofaigh

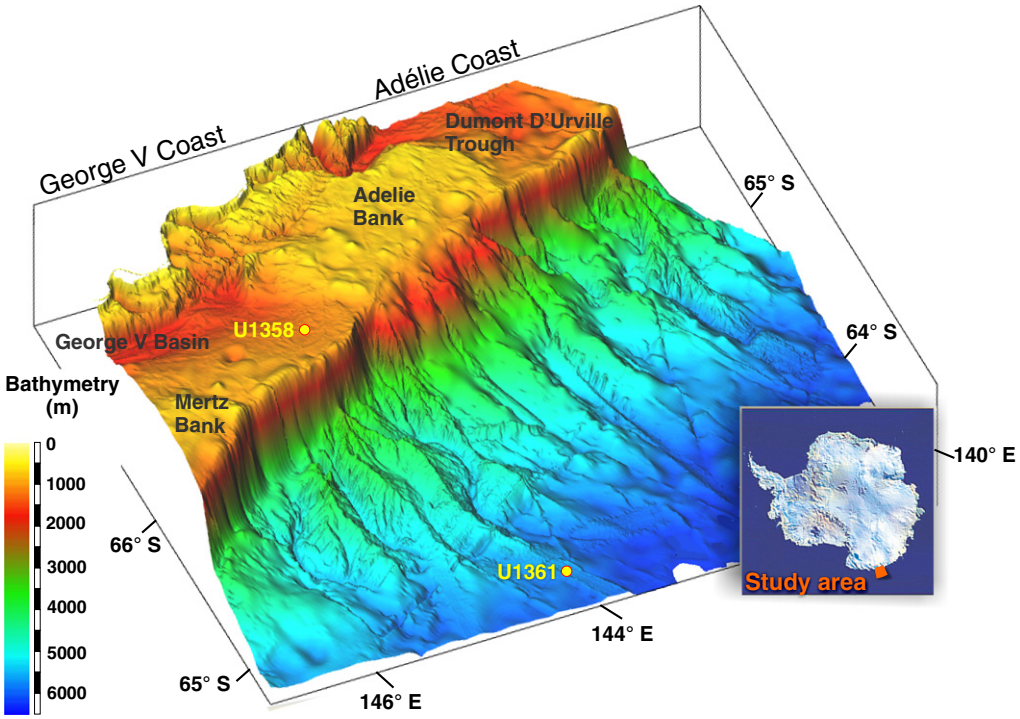

Fig. 1. Bathymetric map showing the location of IODP Sites U1358 and U1361 off-shore from the Adélie Coast within the George V Basin. Modified from Beaman et al. (2010).

et al., 2005; Reinardy et al., 2011a) and to characterise glacimarine sediments (Kilfeather et al., 2010) and iceberg turbates (Linch, 2010).

2D microfabric analyses were used for the entire 6.46 m of cores 3R and 4R using shipboard high resolution digital images of the archive half of the cores and additional thin sections. Microfabric analysis of diamictons is a well-established technique (Chaolu and Zhijiu, 2001; Carr and Rose, 2003; Roberts and Hart, 2005; Stroeven et al., 2005; Thomason and Iverson, 2006; Kalvāns and Saks, 2008). The relationships between the clast microfabrics and other microstructures (e.g. plasmic fabrics, rotation structures, shears, lineations, and water escape structures) can also be examined, providing a detailed microfabric-microstructural map of the thin section (Watling, 1988; Phillips et al., 2011; Vaughan-Hirsch et al., 2012). Individual grains that can be observed in a thin section are known as skeleton grains. Skeleton grains lack a preferred a-axis orientation within glacimarine sediments and thus lack a distinct fabric signal while sediments that have undergone glacial deformation tend to have a clear fabric signal with zones of similarly orientated skeleton grains. Within the current study, microfabric was analysed in a vertical plane, with subglacially derived microfabrics expected to possess a unidirectional or bimodal orientation pattern reflecting a lateral stress field (Carr, 1999, 2001; Carr et al., 2006). However, glacial sediments tend to be polydeformed and Phillips et al. (2011) have shown that in many cases it is possible to interpret several phases of fabric development within the deforming continuum through which tills are deposited. Also crucial is the association of microstructures — in glacimarine deposits these tend to be isolated and unrelated to each other (Carr, 2001; Carr et al., 2006). In contrast, microstructures caused by glacial deformation tend to form in zones or in close association with each other (Reinardy et al., 2011a; Phillips et al., 2011). Thus, evidence from both fabric analyses and microstructures can be effectively combined to interpret differences in glacimarine and subglacial sediments. The analysis of microfabric relating to skeleton grains is particularly important in this context as all the diamictons at Site U1358 have very low clay content and thus do not display any strong directional signal from strial plasmic fabric. Strial plasmic fabric refers to an optical effect of clays when they are closely packed such as is commonly found in subglacial environments, oriented parallel to each other. Viewed in thin section between cross polarisers the aligned clay platelets form birefringent linear zones or domains.

The microfabric data was measured on particles from coarse sand to medium pebbles but is predominantly derived from the very coarse sand and granule size fraction of the sediment. Measurements were also made on skeleton grains down to approximately 20 μm where thin sections were available. A minimum of 50 grain orientations were counted on each of the 20 sedimentary units as defined in the core log in Fig. 2 but normally >150 measurements were made within each unit. The method of Kalvāns and Saks (2008) was followed by splitting the microfabric data set into classes of 10° within rose diagrams. As they note, this is justifiable as the accuracy of the input data is considered to be no better than 10°. Additionally, 10° is the most often used resolution in rose-diagrams in case of till macrofabric studies (Ehlers et al., 1987). Zones of similarly orientated skeleton grains were noted from both the high resolution core scans and in thin section.

3.2. Thin section production

Areas of core 1358B targeted for thin section production followed several criteria. For micromorphological analyses to take place, sediments must be in situ and must not be significantly disturbed by the drilling or sampling process. Thus, only parts of the working half of cores 3R and 4R that were intact could be considered for thin section production. However, since several sections of the core that were of interest were also fragmented or broken, large "mammoth" (150 mm × 80 mm) slides were used so that blocks of sediment from a fragmented part of the core could still be sampled. It is important to note that the blocks were themselves intact and thus preserved the internal structure of the sediments. Care was taken to maintain the stratigraphic position of individual blocks of sediment in relation to each other. Of those intact core sections and sediment blocks, areas where sedimentary structures were visible such as laminae, concentration of grains or matrix rich areas as well as zones of similarly orientated

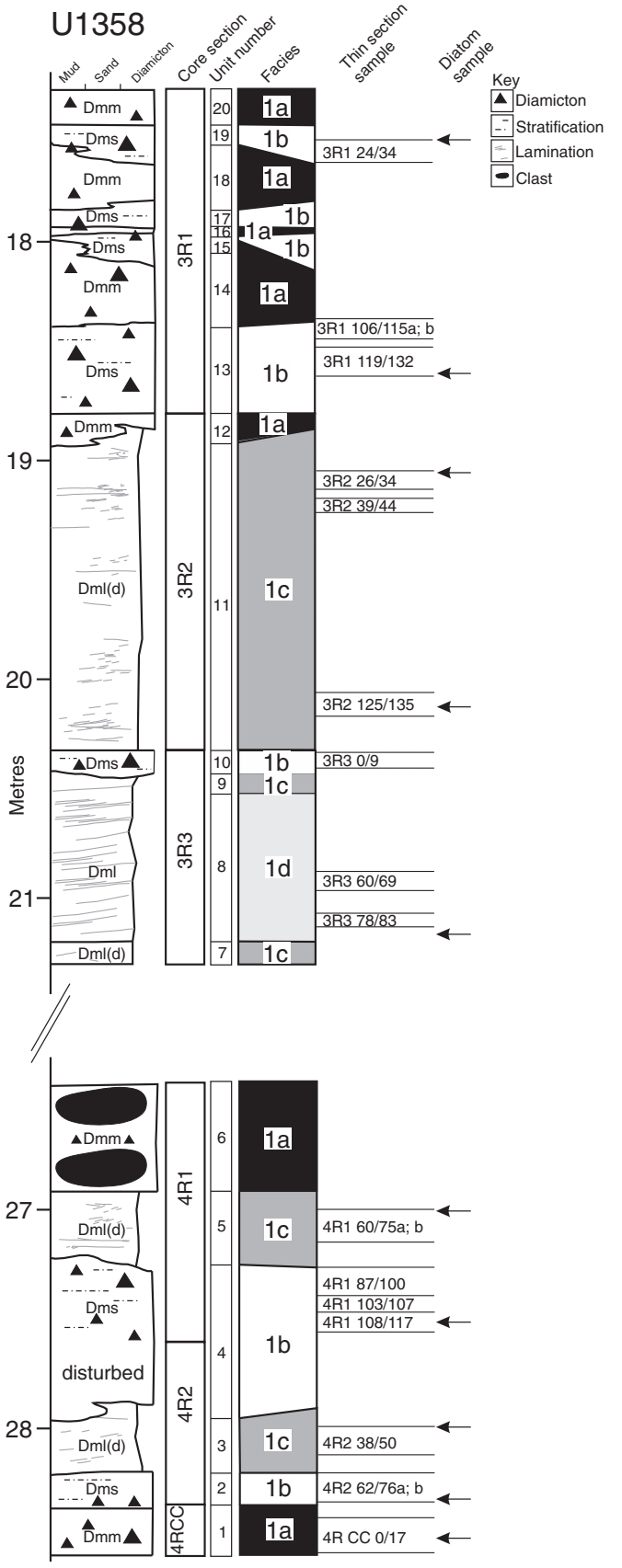

Fig. 2. Stratigraphic log of cores 3R and 4R from Hole 1358B with core sections, sedimentary units and facies interpretations as well as location of diatom samples and thin section sample intervals. The lithofacies code relates to diamictons as follows: Dmm = matrix-supported, massive; Dms = matrix-supported, stratified; Dml = matrix-supported laminated; Dml(d) = matrix-supported, laminated, disturbed. Note two large clasts indicated in unit 6. There was no sediment recovery between 21.54 and 26.4 mbsf.

microfabric (analysed from high resolution scans of the archive half of the core) where targeted along with boundaries between laminated and non-laminated sub-units.

Three thin sections and sixteen large mammoth thin sections were produced sampled vertically in relation to the cores following the techniques set out by Palmer (2005) using an acetone replacement method to dry the samples and avoid sample shrinkage, and sample impregnation with a Crystic resin under vacuum. Because of the consolidated nature of the sediment along with the presence of marine salts, resin impregnation proved particularly challenging. To alleviate this problem, at least five stages of surface impregnation were applied (cf. Kalvāns and Saks, 2008). This was done by smearing a thin layer of resin onto the surface to be used for the thin section, then leaving the sample to dry overnight in a vacuum before sanding the surface with gradually finer sand paper until excess resin was removed and the sediment surface was once again exposed. This process was repeated until the sediment surface remained intact when sanded with fine sand paper. While time consuming, this extra step significantly reduced the amount of material ripped from the surface of samples that had to be ground down to 30 μm thick.

In addition to thin sections, 10 samples were used to analyse diatom assemblages downcore and used to construct a chronological framework for cores 3R and 4R. This was done by placing ~0.01 cm^3 of sediment and a drop of water on a cover slip of 24 × 40 mm and then suspended material was smeared over the cover slip. After this the sample was dried on a hot plate and mounted on a glass slide with UV photopolymer. Abundance of individual taxa was qualitatively estimated from two 22 mm traverses of a smear slide using 630× magnification following the onboard Proceedings of IODP Expedition 318 (Escutia et al., 2011).

4. Results

4.1. Lithostratigraphy and diatom assemblages

The cored interval from 3R-1 down to 4R-CC extends from 17.3 to 35.6 mbsf. Within this interval, 6.46 m of sediment was recovered (Fig. 2). Diatoms are relatively rare with total number of diatoms per smear slide ranging from 53 to 110. Preservation in terms of fragmentation is poor but it was still possible to identify a total of 45 taxa (Fig. 3). No significant changes of diatom abundance and assemblage have been observed in our samples downcore.

Initial shipboard analysis (Escutia et al., 2011) described cores 3R and 4R consisting of only one unit of diamicton and diamictite that transitions between grey clast-rich muddy and clast-rich sandy composition. On-board clast abundance was visually estimated at between 5% and 7.5% although this estimate is probably too low as it likely relates to clasts >0.5 cm. Careful inspection of the high resolution core scans reveals greater concentrations of smaller clasts < 0.5 cm particularly in sedimentary units described below. The largest clasts are up to 26 cm. Clast lithologies are variable and include basalt, granitic gneiss, quartzite, and fine-grained metasediments (Escutia et al., 2011). Clasts have subangular to subrounded shapes and basalt and metasedimentary clasts are often faceted and occasionally striated and fluted. Orejola et al. (2014) carried out grain size distribution on both cores 3R and 4R, with 3R having a mainly unimodal distribution while 4R displayed a bimodal distribution.

Cores 3R and 4R are divided into 20 sedimentary units based on their macro-scale structures and microstructures (Figs. 4A to C, 5A to D and 6A to B) as well as measured fabric characteristics (Figs. 7 and 8). Core section 4R-CC consists of unit 1 (Fig. 2). There is a strong directional signal from the microfabric between 30° and 40°. Thin section 4R CC 0/17 sampled this unit and displays an uneven skeleton distribution as well as lineations made up of aligned skeleton grains. Occasionally, some of the individual skeleton grains that make up the lineations are fractured (Fig. 4C). There are some grain stacking features that are

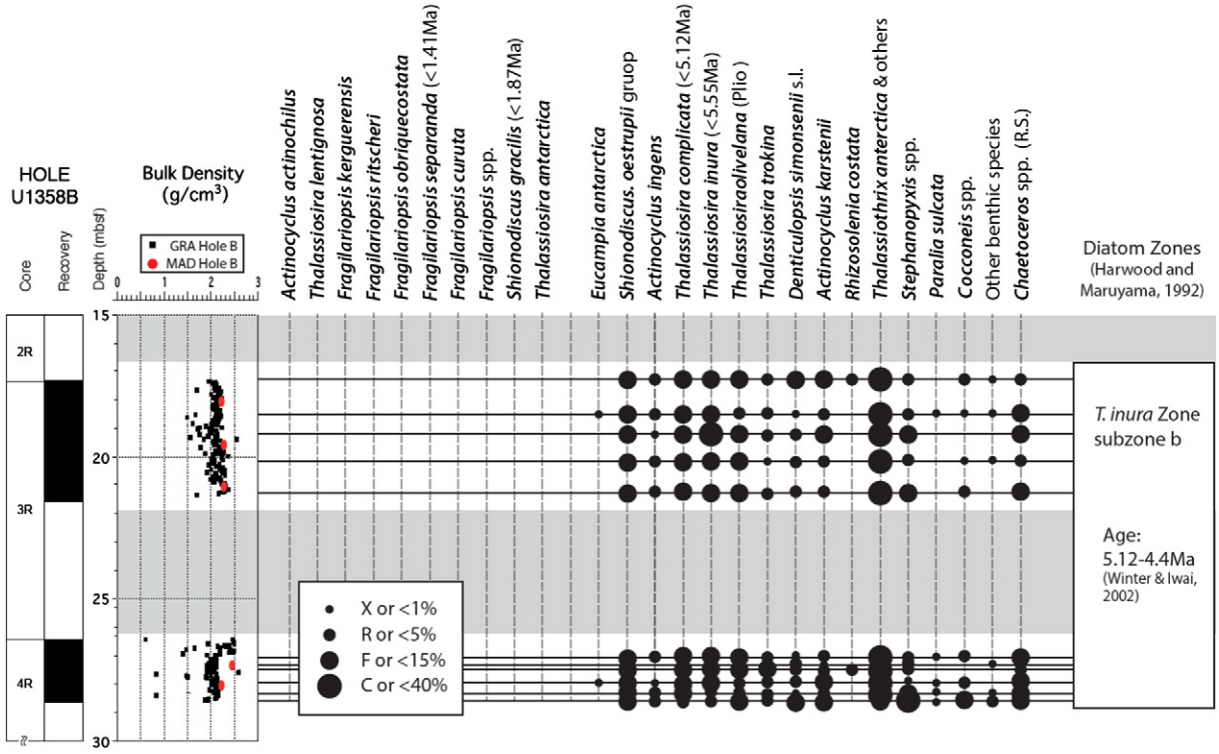

Fig. 3. Diatom assemblage for cores 3R and 4R indicating an early Pliocene age between 4.1 and 5.12 Ma.

made of skeleton grains that have parallel a-axes. Rotation structures were also observed in thin section 4R CC 0/17 that comprise a circular, tangential arrangement of skeleton grains with, or without, a central core grain formed by a larger clast (Phillips, 2006; Lea and Palmer, 2014). In some situations, rather than a circular arrangement of skeleton grains there is a zone of fine matrix immediately adjacent to either a core grain or intraclast (Fig. 4C). These intraclasts consist of finer dark brown or grey material. This finer matrix also forms what appear to be water escape features that cross-cut the microfabric (Fig. 4C).

Core section 4R-2 contains units 2 and 3 (Fig. 2). The upper part of this core section has been disturbed and only small broken blocks of sediment remain which have been included as part of unit 4 described in core section 4R-1. Units 1 and 2 have been separated because there is a bimodal fabric signal in unit 2. The S1 fabric is orientated between 130° and 160° while the S2 fabric is orientated between 35° and 50° (see Section 5.2 for explanation of S1 and S2 fabrics). This range of orientations also applies to all other units that have S1 and S2 fabrics (Fig. 7). Thin sections 4R2 62/76a and 4R2 62/76b that sampled unit 2 both contain rotation structures mainly lacking core grains but when core grains are present they tend to be surrounded by matrix "halos" rather than individual skeleton grains (Fig. 5B). Both intraclasts and water escape structures were present along with lineations of individual skeleton grains. Features such as water escape structures, intraclasts and rotation structures are more common and better preserved than lineations of skeleton grains (Table 1). Unit 3 has a very even skeleton grain distribution but no distinct fabric orientation. Disrupted laminae and bedding are observed in thin section 4R2 38/50.

The base of core section 4R-1 comprises units 4 to 6 (Fig. 2). Thin section 4R1 108/117 sampled the lower part of unit 4 and contains both circular structures and intraclasts (Table 1) occasionally in proximity to cracked grains. Thin section 4R1 87/100 sampled the upper part of unit 4 where zones of skeleton grains with similarly orientated a-axes are cross-cut by large water escape structures (Fig. 5D). Indistinct discontinuous bedding at mm-scale, dip at varying angles within unit 4. Unit 5 has disrupted laminae seen in thin sections 4R1 60/75a and 4R1 60/75b (Fig. 6B) where occasionally it is possible to observe poorly or partially developed rotation structures and isolated, variably orientated grain lineations (Fig. 6A) but no distinct fabric orientation. At a micro-scale the laminae are picked out by their slightly higher birefringence in comparison to the surrounding matrix (Fig. 6B). To the left of the photomicrograph in Fig. 7A the individual lamina is slightly deformed or disrupted and a thin fissure can been seen within the lamina. Grain stacks are also present in unit 5 (Fig. 6A). Unit 6 contains 3 large clasts up to 26 cm with a thin 5 cm layer of sediment between these clasts (Fig. 2). Despite the limited exposure, it was possible to make 64 fabric orientation measurements in unit 6 which indicated the presence of S1 and S2 fabrics.

Core section 3R-3 contains units 7 to 10 (Fig. 2). Units 7 and 9 contain disrupted laminae while in unit 8 prominent laminae are between 1 and 5 mm thick and tend to dip between 40° and 60° (Fig. 8). The a-axes of many of the clasts > 1 cm tend to dip in the same direction. The laminae can be picked out on the core scans by their lighter brown colour in comparison to the surrounding matrix however sometimes the laminae are cross-cut by grey sediment layers < 0.5 cm thick dipping at 290° to horizontal (Fig. 8). A vast majority of skeleton grains are subrounded. There is no distinct fabric orientation in unit 7, 8 or 9 (Fig. 8). Unit 10 is sampled in thin section 3R3 0/9 and has a fabric signal as well as rotation and lineation structures (Table 1).

Core section 3R-2 contains unit 11 and 12 (Fig. 2). Unit 11 has disrupted laminae, even skeleton grain distribution but no distinct fabric orientation and isolated rotation structures as indicated in thin sections 3R2 125/135, 3R2 39/44 and 3R2 26/34 (Table 1). Unit 12 has zones of orientated fabric and lineations of skeleton grains as well as smeared zones of fine to medium sand.

Core section 3R-1 contains units 13 to 20 all of which have grain lineations (Figs. 4A, B and 5A), intraclasts (Fig. 5C) and rotation structures (Figs. 4A and 5A). In units 13, 15, 17 and 19 these rotation structures tend to mainly be made up of thick "matrix coats" around a core grain (Fig. 4A) while in units 14, 16, 18 and 20 they tend to form haloes (Fig. 5B) and occur both with and without core grains sometimes with two layers of skeleton grains formed around the core grain (Fig. 5A). Units 13 to 20 all contained both S1 and S2 fabrics (Fig. 7).

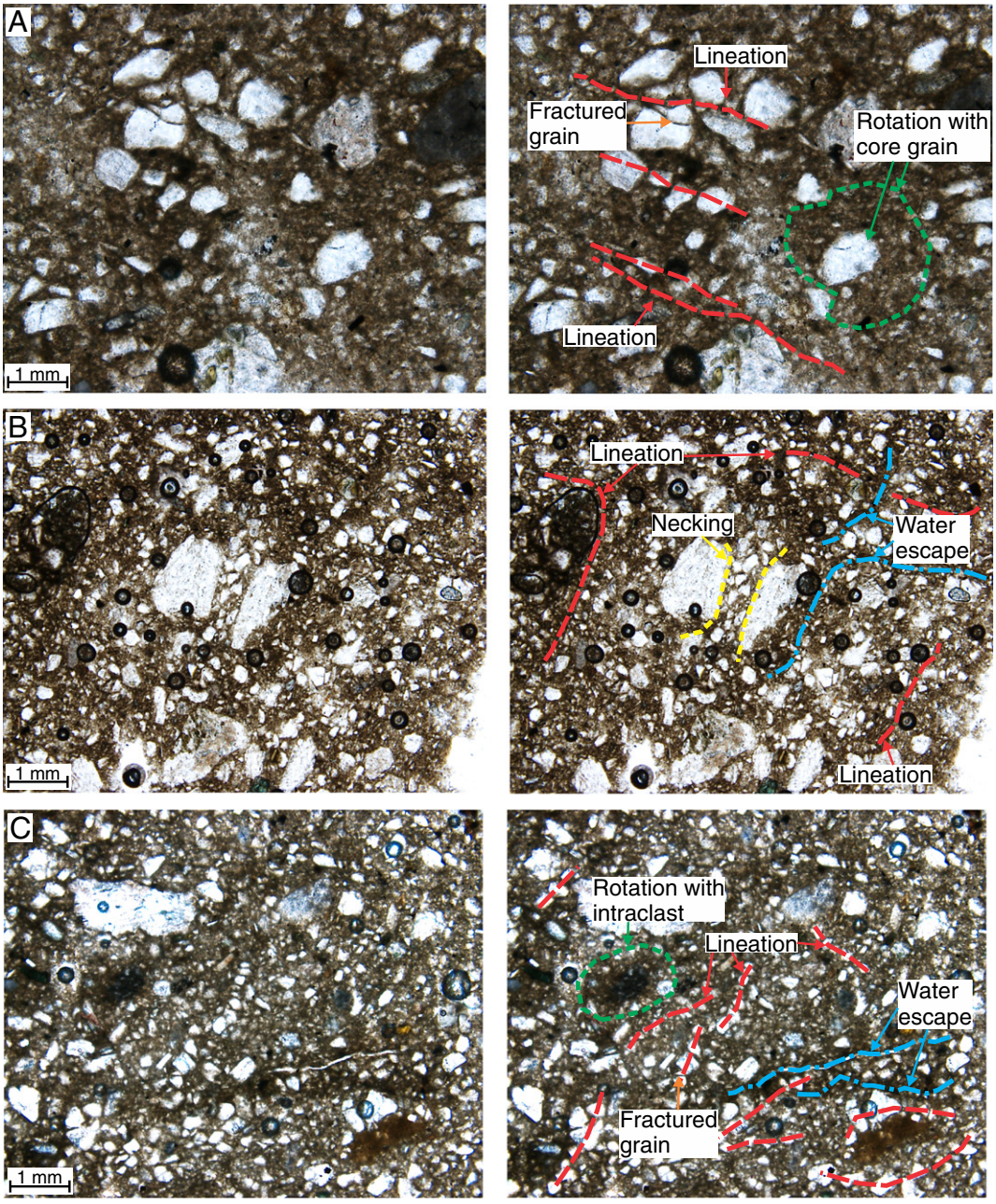

Fig. 4. Photomicrographs from facies 1a with and without annotation, see Fig. 2 for location of thin section samples. A) From thin section 3R1 106/115a showing rotation structure with core grain surrounded by a matrix coat outlined by the green dashed lines. Lineations indicated by red dashed lines made up of individual skeleton grains in proximity to fractured grain (orange arrow). Note fracture is infilled with matrix. B) From thin section 3R1 24/34 showing necking structure between large skeleton grains (dashed yellow line) with possible water escape structure (blue dot dash line). C) Taken from thin section 4RCC 0/17 showing intraclast with rotation structure made up of fine matrix material (green dashed line) in proximity to grain lineations. Some of the individual grains that make up the lineations are fractured (orange arrow) and water escape structures are also indicated.

Unit 13 sampled in the bottom of thin sections 3R1 106/115a and 3R1 106/115b contained necking structures (Fig. 4B) and pressure shadows (Fig. 5C) while the top of the thin sections sampled unit 14 that contained cracked grains (Fig. 5A). In unit 19, thin section 3R1 24/34 contained rotation structures both with and without core grains that were made up of both skeleton grains and matrix coats.

5. Interpretation

5.1. Depositional settings for U1358

We have interpreted four different depositional facies within units 1 to 20, these are facies 1a to 1d (Fig. 2). The technique of McKay et al. (2009) is used where variations in lithofacies primarily reflect changes in depositional energy that in turn reflects changes in glacial proximity. The units are normally not separated by sharp erosional contacts as was observed for the glacimarine units at the AND-1B site (McKay et al., 2009), because either it was not possible to recover the interglacial diatomaceous units similar to those found at AND-1B or they were removed at Site U1358B by glacial reworking during ice advance. Either way it is very likely that hiatuses exist within our record.

5.2. Facies 1a and 1b

Facies 1a and 1b are interpreted as having been deposited in a subglacial or grounding line proximal environment (Fig. 2). Facies 1a

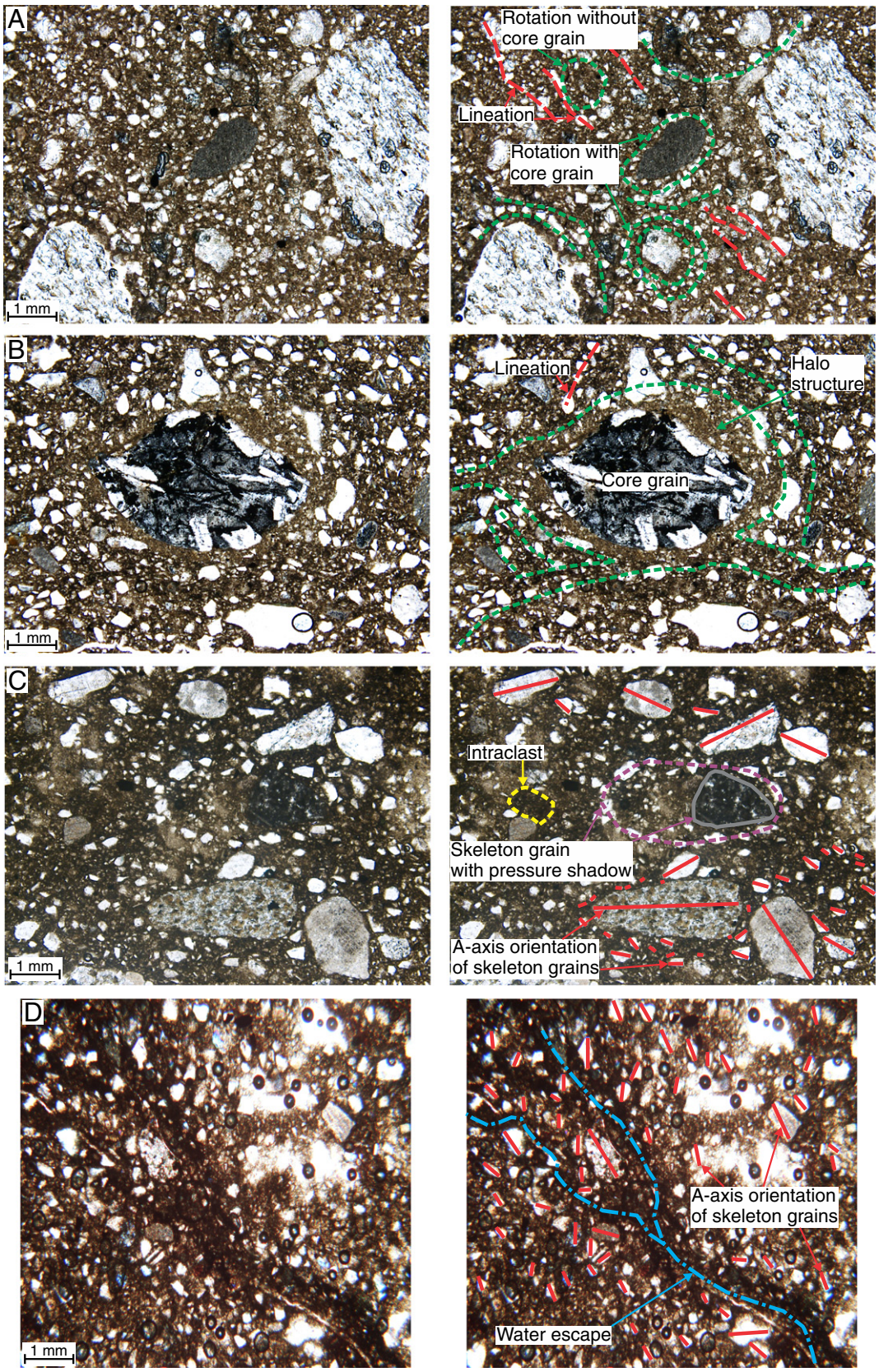

Fig. 5. Photomicrographs from facies 1b with and without annotation, see Fig. 2 for location of thin section samples. A) From thin section 3R1 24/34 showing rotation structures with and without core grain (green dashed lines) and lineations of individual skeleton grains (red dashed lines). B) Taken from thin section 4R2 62/76a showing large skeleton grain with halo structure (green dashed line) made up of finer matrix material that has a slightly higher birefringence than the surround matrix. C) Taken from thin section 3R1 106/115b showing skeleton grain (outlined in grey) with pressure shadow (purple dashed line) made up of smaller skeleton grains in proximity to intraclast (yellow dashed line). D) Taken from thin section 4R1 87/100 within S2 fabric zone intersected with water escape structure (blue dot dash line).

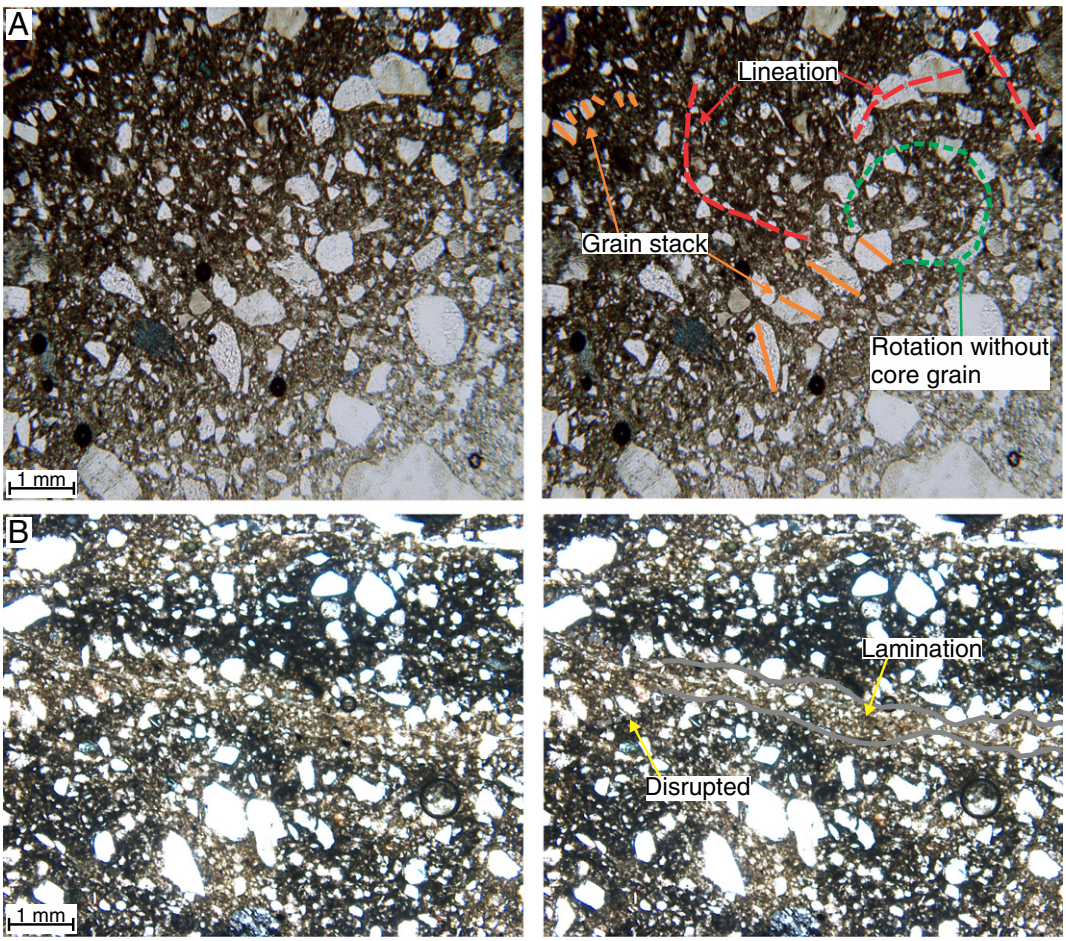

Fig. 6. Photomicrographs from facies 1c with and without annotation, see Fig. 2 for location of thin section samples. A) From thin section 4R1 60/75a showing poorly developed rotation without core grain (green dashed line), lineations (red dashed lines) made up of finer grains and individual skeleton grains and grain stacks indicated in orange. B) From thin section 4R1 60/75b with black line outlining individual lamina that is partially disrupted to the left of the photomicrograph. Note the lamina has a higher birefringence than the surrounding matrix.

and 1b are similar; both are massive, grey to greyish brown, matrix-supported and have zones of weak to moderate similarly orientated fabrics (Fig. 7). A majority of clasts are < 0.5 cm but there is also a significant number of clasts between 0.5 and 1.5 cm. These larger clasts are more common in facies 1b along with zones where clast concentration is comparatively higher (but still matrix-supported). In contrast, facies 1a tends to be more matrix-rich. Importantly, both facies have a preferred fabric orientation that is either unimodal or bimodal (referred to as S1 and S2 fabrics) which is common in polydeformational tills formed within a deforming continuum and increasing stress regime but would not be expected in sediment deposited in open marine conditions or via mass movement (Carr et al., 2006; Phillips, 2006, 2011; Reinardy et al., 2011a). S1 fabric (orientated between 130° and 160°) is formed before S2 fabric (orientated between 35° and 50°) so S1 fabric is not always preserved or has limited preservation. This means that while nearly all the measured clasts within a unit fall into two orientation ranges (giving a distinct bimodal signal), a higher number will fall into the S2 fabric orientation range because it is better preserved compared to the S1 fabric range. In addition, even within an individual sedimentary unit that has a bimodal fabric signal, it is sometimes possible to identify zones where either the S1 fabric is particularly strong or more commonly where the S2 fabric is strong (Figs. 5D and 7). These zones tend to be more common in facies 1b because it is less homogenised in comparison to 1a and areas of facies 1b where these zones are not apparent may be due to reworking by processes such as debris flows (see the contrast between the upper and lower portions of facies 1b in Fig. 7). The zones of fabric orientation may have been caused by shearing along discrete shear planes (sometimes localised and short-lived) within the deforming till (Larsen et al., 2007). Mechanical properties of the sediment along with grain size distribution determine the thickness of shear zones (Hicock et al., 1996; Stroeven et al., 2005; Thomason and Iverson, 2006). Thus, well-sorted sediments tend to have a stronger microfabric signal because shear zones will be more uniform (Carr and Rose, 2003; Kalvāns and Saks, 2008). The diamicts sampled from the lower part of core 3R by Orejola et al. (2014) have a primarily unimodal particle-size distribution and consist of glacimarine sediments. These sediments would have been reworked during grounded ice advance and deposition of facies 1a and 1b in the upper part of core 3R and this may explain the strength of the microfabric signal i.e. the preferred orientation of the clasts, observed in facies 1a and 1b in core section 3R-1 (Fig. 7).

Both facies also contain evidence of polydeformational microstructures commonly associated with subglacial tills (Figs. 4A to C and 5A to D) (van der Meer, 1993; Menzies, 2000). However, facies 1a tends to appear far more homogenised at a micro-scale and tends to have a lower concentration of structures in comparison to facies 1b (Fig. 4A to C, Table 1). This type of homogenisation and limited preservation of microstructures, particularly brittle deformation structures, is common in subglacial tills (Reinardy et al., 2011a and the references therein). Thus, facies 1a is interpreted as a grounded ice unit that has likely undergone prolonged subglacial deformation either during a single or multiple glacial cycles. Because facies 1b is not as homogenised as facies 1a, preservation of microstructures is increased (Fig. 5A–D). In addition, some of the microstructures may actually have formed by processes

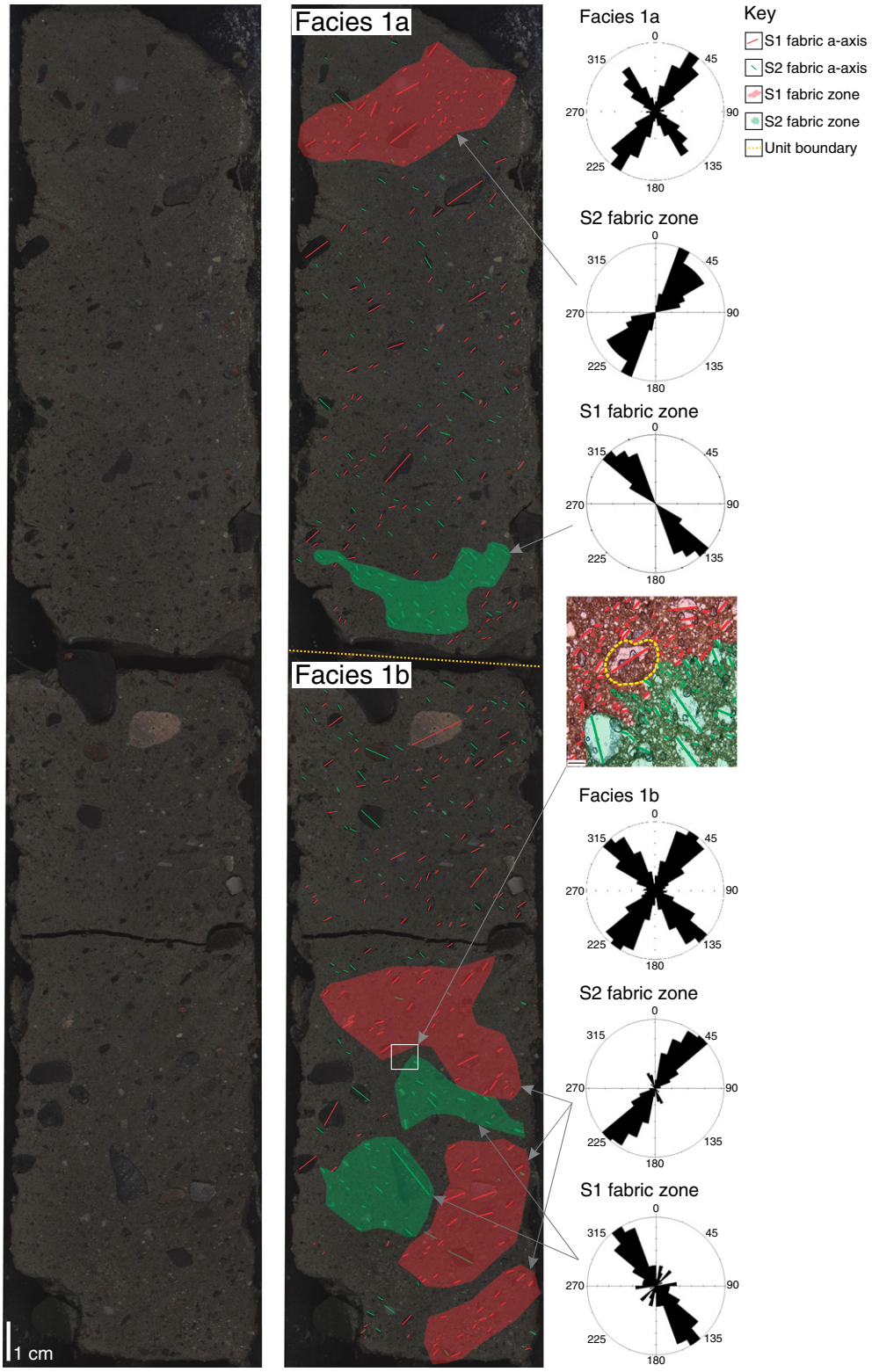

Fig. 7. High resolution scan of core 3R Section 1 from 0 to 34 cm with annotation on the right showing a typical example of facies 1a and 1b (units 19 and 20) with the boundary marked by dashed yellow line. Red lines indicate clasts with an a-axis orientated between 35° and 50° (S2 fabric) and green lines indicate clasts orientated between 130° and 160° (S1 fabric) highlighting that a majority of clast fall within these orientations. In some areas there is a grouping or zone of S2 fabric (red shaded area) or S1 fabric (green shaded area). The photomicrograph on the right is from thin section 3R1 24/34 and shows the boundary between a zone of S2 fabric (which also contains a rotation structure indicated in yellow) and S1 fabric (location indicated by white box, scale bar = 1 mm). The rose diagram labelled facies 1a relates to all a-axis orientation measurements from units 1, 6, 12, 14, 16, 18 and 20. The rose diagram labelled facies 1b relates to all a-axis orientation measurements from units 2, 4, 10, 13, 15, 17 and 19. Additional rose diagrams relate to shaded S1 and S2 fabric zones indicated by arrows.

Fig. 8. High resolution scan of core 3R Section 3 from 59.5 to 105.5 cm with annotation on the right showing typical examples of facies 1d and 1c with the boundary marked by a dashed yellow line. The rose diagram labelled facies 1c relates to all a-axis orientation measurements from units 3, 5, 7, 9 and 11. The rose diagram labelled facies 1d relates to all a-axis orientation measurements from unit 8. Grey lines indicate laminae and purple lines indicate possible diagenic layers.

Table 1
Micromorphological description and comparison of thin section samples (cf. Carr, 1999). The presence of a single dot identifies the presence of a particular feature, while two or three dots indicate much clearer, or more common structures. Key to matrix textures: M = medium (some fine silt and clay); F = fine (abundant silt and clay). See text for explanation of different types of rotation structures.

Thin section	Facies	Skeleton to matrix ratio	Skeleton distribution	Matrix texture	Necking	Cracked/fractured grains	Lineations	Circular structure, core grain	Circular structure, no core grain	Circular structure matrix	Circular structure (matrix and skeleton grains)	Grain stacking	Zones of skeleton grains with orientated a-axis	Intraclasts	Pressure shadows	Water escape	Galaxy structures
3R1 24/34	1b	Skeleton rich	Uneven	F	●●	●	●●	●●	●	●	●		●				
3R1 106/115a	1a/1b	Matrix rich	Even	F		●●	●		●					●			
3R1 106/115b	1a/1b		Even	M			●		●		●			●	●	●	
3R1 119/132	1b		Even	M	●		●●		●●				●●	●●			●
3R2 26/34	1c	Skeleton rich	Even	M			●●	●●	●●			●●	●	●		●●	
3R2 39/44	1c	Skeleton rich	Even	M			●	●					●●	●		●●	
3R2 125/135	1c		Even	F			●●	●●	●●	●●		●●	●●		●	●●	●
3R3 0/9	1b		Uneven	M			●●●		●●			●●	●●		●●	●●	
3R3 60/69	1d	Matrix rich	Even	F					●								
3R3 78/83	1d	Matrix rich	Even	F												●	
4R1 60/75a	1c			F	Yes		●●		●●			●●	●●				
4R1 60/75b	1c		Uneven	F			●●			●●			●●	●●	●	●●	
4R1 87/100	1b	Skeleton rich	Uneven	F			●			●●			●●			●●	
4R1 103/107	1b		Uneven	M			●●	●	●							●●	
4R1 108/117	1b			F		●●	●●	●●	●●	●●				●●			
4R2 38/50	1c	Skeleton rich	even	F				●●						●●	●		
4R2 62/76a	1b		Uneven	M	●		●●		●●	●●	●	●●		●●		●●	
4R2 62/76b	1b		Uneven	M			●		●							●	
4R CC 0/17	1a		Uneven	M		●●	●●●				●●	●●	●				

such as sediment debris flows or melt-out of debris-rich basal ice (cf. Powell and Cooper, 2002; Presti et al., 2005). This could explain the prevalence of water escape structures (Fig. 5D), but also the variable types of rotation structures observed in facies 1b (Lea and Palmer, 2014) (Fig. 6A, B, Table 1). Previous work has suggested that these sorts of microstructures can be caused by turbulent flow within debris flows (Phillips, 2006; Reinardy and Lukas, 2009). In addition, there are occasional clustering of larger clasts across core giving the impression of flow plus occasional poorly developed stratification identified by thin (<0.5 cm) layers of fine grey matrix which is distinct from the greyish brown matrix in other parts of the unit. The variation in matrix colour may relate to stratified areas containing a slightly higher clay or silt content but these features tend to be very subtle.

Homogenisation of deformation tills particularly at the bed of fast flowing outlet glaciers occurs relatively rapidly within a deforming continuum. Thus, facies 1b likely represents deposition as the grounding line was directly over the core site or slightly advanced beyond the core site. It is also possible that facies 1b may well have been deposited when the grounding line was landward but proximal to the coring site just before grounded ice arrived because processes such as debris flows and debris-rich basal melt-out could have distributed subglacially modified material directly in front of grounding line as well. However, where zones of S1 and S2 fabrics are observed within facies 1b as shown in the lower section of 1b in Fig. 7 then a debris flow scenario is less likely. The generations of brittle and ductile deformation structures sometimes make it possible to make a tentative interpretation as to whether the grounding line was likely to be advancing or retreating as facies 1b was being deposited.

5.3. Facies 1c and 1d

Facies 1c and 1d are interpreted as grounding line distal to open marine deposits as both are matrix-supported and are finely laminated (Figs. 6B, 8) (Domack, 1982, 1988; Harris et al., 2001; Ó Cofaigh and Dowdeswell, 2001; Powell and Domack, 2002; McMullen et al., 2006; McKay et al., 2009; Orejola et al., 2014). Both facies lack any clear directional signal in their fabric data (Fig. 8). At a micro-scale the laminae are more birefringent in comparison to their surrounding matrix (Fig. 6B) although the lack of zones of birefringent matrix (plasmic fabric) indicates that overall clay content within 1358B is low. While the majority of the laminae are made up of finer matrix material, individual skeleton grains can also be observed encased within the individual laminae (Fig. 6B). The laminae along with some of the larger clasts tend to dip across core and in some cases such as those in Fig. 8 the dip can be as steep as 60°. This is not thought to be a primary depositional feature. Passchier (2000) describes similar dipping bedding and laminae in cores from Cape Roberts and interpreted this as evidence of soft sediment deformation from slumping in an ice-distal fjord environment. It is possible that the laminae at 1358B have undergone similar post-depositional soft sediment deformation but the site of U1358 is on the outer shelf and the laminated units occur both directly below and above sediments deposited by grounded ice. Therefore, it is more likely that the apparent dip of the laminae has been caused by post-depositional glacitectonic effects due to the numerous glacial cycles that would have overrun the area up until the Last Glacial Maximum. Glacitectonism is a common feature of sediments deposited on previously glaciated shelves and is caused by overriding ice deforming underlying substrate (Lee and Phillips, 2013). It is likely that the rare deformation structures in facies 1c probably relate to post-depositional processes such as loading causing grain stacks (Fig. 6A) or small-scale grain flows or slumping forming poorly developed rotation structures and grain lineations although some of these features could also be inherited. It should be noted that while facies 1c includes features such as poorly developed rotation structures, they are considerably different in appearance when compared to the well developed rotation structures found in facies 1a or 1b (compare rotation structure in Fig. 6A from facies 1c with rotation structure in Fig. 5A and B from facies 1b). In addition, facies 1c has no preferred fabric orientation in stark contrast to facies 1a and 1b (Fig. 5D). The fact that both facies 1c and 1d are at least partially laminated suggests that the disruption of these units by processes such as iceberg scouring has not been significant (Barnes and Lien, 1988; Linch et al., 2012).

Taking into account that changing lithofacies is likely to mean changing depositional energy relating to position of the grounding line (cf. McKay et al., 2009), it is tentatively suggested that while both facies 1c and 1d were deposited distal to the grounding line, the grounding line was closer to Site U1358 during the deposition of facies 1c in comparison to 1d. The stratification, water escape structures and disruption to the laminae along with the coarser nature of facies 1c may relate to meltwater plumes or the interaction of strong bottom currents followed by small-scale grain flows as highlighted in Prydz Bay.

5.4. Facies interpretation of core 4R

Section 4R-CC, consists of unit 1 and shows evidence of subglacial deformation and has been interpreted as facies 1a (Fig. 2). Deformation would have occurred as ice moved over the substrate but also as sediment was advected downstream (cf. Reinardy et al., 2011a,b). It represents the oldest unit stratigraphically and records the first grounded ice event in the record (Fig. 2). There is a strong directional signal from the microfabric between 30° and 40° which would be expected in a uniform tensional or compressional stress regime (Carr and Rose, 2003). This is in contrast to the progressively changing grain orientations observed in all the other ice contact units described within core 4R and 3R that have both S1 and S2 fabrics. It is probable that the evidence of the older S1 fabric has not been preserved. The core sections are not orientated at Site U1358 so it is not possible to say whether microfabric is parallel or transverse to ice flow direction, but in this case it is suggested that they are more likely to be aligned transverse. This is because grains aligned transverse to ice flow direction are affected by a much higher total stress than those where grains are aligned parallel to ice flow direction (Taylor Rotation versus Jeffery Rotation, Carr and Rose, 2003). Because there is evidence of cracked and fractured grains from thin section 4R CC 0/17 the higher stress state is more probable (Fig. 4C). This would also explain why the S1 fabric has not survived. Fractured and cracked grains have previously been shown to relate to brittle failure with subglacial shearing (indicated by grain lineations) followed by sediment dilation (Hiemstra and van der Meer, 1997). The uneven skeleton distribution and circular structures indicate rotation of individual grains also caused by shearing but this time within a ductile deforming sediment mass (van der Meer and Menzies, 2011 and the references therein). The presence of intraclasts (Fig. 4C) suggests ductile deformation but water escape features that cross-cut the microfabric probably relate to dewatering after dilation of the sediment as is commonly found in tills (e.g. Reinardy et al., 2011a). It is important to note that even in cold polar glacial regimes significant amounts of subglacial meltwater may still be present (Lowe and Anderson, 2002; Bælum and Benn, 2011; Reinardy et al., 2013). The greyish or dark brown sediment that makes up the intraclasts probably relates to reworked glacimarine sediments (Fig. 4C). Reworking of underlying sediment and clastic intrusions was observed within subglacially deformed units within the AND-1B core (McKay et al., 2009). Grain stacking probably relates to post-depositional loading of the sediment.

Following the initial advance of ice (unit 1), unit 2 is interpreted as facies 1b and was deposited either as ice retreated from the site or possibly related to another grounded ice event (Fig. 2). It is not possible to say whether the bimodal fabric signal in unit 2 represents individual deformation events or whether they are part of the same event within a single deforming continuum. This is because, as mentioned above, even during a single event, grains will initially orientate themselves parallel

to the ice flow direction but continued stress causes smaller grains to become orientated transverse to ice flow direction. Well developed rotation structures with halos (Fig. 5B), intraclasts and water escape structures all suggest ductile reworking along with lineations of individual skeleton grains, which indicate shear. The subtle difference in the preservation of slightly more distinct ductile structures compared to brittle microstructures indicates that final deformation of the sediment may have been initiated by increased saturation possibly as ice melted at the grounding line as grounded ice retreated from the site (Table 1).

Unit 3 is partially laminated and has a very even skeleton grain distribution indicative of open marine conditions rather than subglacial deposition where clustering of skeleton grains commonly occurs (Carr, 2001; van der Meer and Menzies, 2011). Thus, unit 3 is interpreted as facies 1c. The top of core section 4R-2 has been significantly disturbed during recovery and it is not possible to make any firm interpretations although it may be part of unit 4 above.

The base of core section 4R-1 (unit 4) is interpreted as facies 1b and indicates the return of grounded ice (Fig. 2). At the base of the unit, thin section 4R1 108/117 contains both circular structures and intraclasts (Table 1) indicating flow and rotation of skeleton grains that probably relate to subglacial deformation because they occur in close association with cracked grains. Evidence of brittle deformation and shear is rare which probably reflects limited preservation potential within a grounding line proximal environment. Facies 1b in unit 4 was likely deposited during retreat of grounded ice. Evidence for this is observed at the top of the unit sampled in thin section 4R1 87/100 where zones of skeleton grains with similarly orientated a-axes are related to subglacial deformation but cross-cutting these zones are large water escape structures that relate to deformational processes post initial subglacial modification probably involving small-scale debris or gravity flows (Fig. 5D) (Reinardy and Lukas, 2009). Indistinct discontinuous bedding at mm-scale, dip at varying angles which may represent the base of small debris flow units or thin slurry layers that can occur at the surface of mass flow units (Phillips, 2006; Reinardy and Lukas, 2009). This type of poorly developed stratification within diamictons has previously been interpreted as debris flows that have partially sheared the tills (Hiemstra et al., 2004).

Unit 5 is laminated and has been interpreted as facies 1c. The laminae may have been disrupted during the deposition of unit 6 by grounded ice directly above as discussed earlier. Fig. 6B shows the partial disruption to an individual lamina to the left of the photomicrograph where the lower boundary of the lamina appears to be partially amalgamated into the surrounding matrix. Additional post-depositional or inherited features can be observed in thin sections 4R1 60/75a and 4R1 60/75b where occasionally it is possible to identify poorly or partially developed rotation structures and isolated, variably orientated grain lineations (Fig. 6A). It is important to note however that the laminae such as those shown in Fig. 6B indicate that the deformational features mentioned above and shown in Fig. 6A are unlikely to have formed in a subglacial environment. The thin fissures that in some cases can be observed within and running parallel to the laminae are related to desiccation during thin section production (Palmer, 2005). While siliceous microfossils are rare and relatively poorly preserved throughout core 4R, unit 5 does have a slightly higher concentration than units directly above and below, which also suggests open marine conditions during this period (Escutia et al., 2011). Thin sections 4R1 60/75a and 4R1 60/75b both contain features similar to grain stacks (Fig. 6A). Normally these features contain at least five equally sized grains that are partially crushed or fractured and are found in subglacial environments (Larsen et al., 2007). However in our samples none of the grains show signs of fracturing and possibly relate to loading rather than subglacial deformation. Loading may have occurred during dewatering of the sediment that was clearly highly saturated at one point (as would be expected in open marine conditions). A bimodal grain-size distribution with enrichment in sand and some sorting in this part of core 4R led Orejola et al. (2014) to interpret a glacimarine depositional environment influenced by current activity. The presence of S1 and S2 fabrics in unit 6 indicates a return to glacial conditions during this part of the record and may also explain the disruption to laminated units below but this interpretation is tentative because of the disturbed nature of the unit.

5.5. Facies interpretation of core 3R

3R-3 is the most distinct section of both cores 4R and 3R. This is due to prominent laminae in unit 8 which is interpreted as facies 1d (Fig. 8). Units 7 and 9 were also deposited in open marine conditions and are interpreted as facies 1c. Units 7 to 9 are similar to many glacimarine units from other polar marine environments (Licht et al., 1999). Thin sections 3R3 78/83 and 3R3 60/69 from unit 8 have no preferred fabric orientation and core sections 3R3 and 3R2 have a unimodal grain-size distribution that also indicates glacimarine deposition (Orejola et al., 2014). It is also worth noting that a vast majority of skeleton grains are subrounded (Fig. 8) in comparison to ice contact sediments that tend to contain a greater variety of clast forms (Carr et al., 2006). Sometimes the laminae are cross-cut by thin grey sediment. The origin of these features is uncertain as they were not sampled in thin section but they could be diagenic because while they cross-cut the laminae there is no displacement (Fig. 8). There does not appear to be a change in grain size within the grey layers either.

There is the possibility that the 9.5 cm thick unit 10 at the top of core section 3R-3 represents a return to grounded ice conditions although our interpretation of the unit as facies 1b is only tentative (Fig. 2). This interpretation is based on thin section 3R3 0/9 that shows a fabric signal in contrast to thin section 3R3 60/69 below from unit 8 that lacks any directional signal. Thin section 3R3 0/9 also contains both rotation and lineation structures (Table 1).

Section 3R-2 mainly consists of unit 11 interpreted as facies 1c (Fig. 2). It is very probable that the disruption of this thick laminated unit was caused when the site was overrun by grounded ice for a significant period that is represented by subglacial units above. Unit 12 has been interpreted as facies 1a and marks the onset of subglacial and grounding line proximal conditions that last throughout the stratigraphically youngest part of our record. The smeared zones of fine to medium sand may have been reworked from the open water deposits below.

Section 3R-1 contains alternating facies 1a and 1b indicating repeated grounding line proximal to grounded ice conditions over the site when units 13 to 20 were deposited that either prevailed during the entire period or where separated by grounding line distal/open marine conditions but these units were not preserved (Fig. 2). Both facies contained grain lineations (Figs. 4A to C and 6A), intraclasts (Figs. 4C and 5A, C) and rotation structures. The differences between rotation structures within facies 1a with “matrix coats” with core grains (Fig. 4A) and facies 1b both with and without core grains defined by “halos” (Fig. 5B) or occasionally both skeleton grains and matrix coats surrounding a core grain (Fig. 5A) probably relate to different levels of reworking experienced by both facies (Lea and Palmer, 2014). Their association with grain lineations (Figs. 4A, C and 5A) probably represents the changing processes with which strain is accommodated within sediment with varying porewater concentrations (Phillips et al., 2011, 2012; Carr and Rose, 2003).

The interpretation of some of these alternating units is tentative because although clast fabric was measured, it was not possible to sample all the units in thin section. Units 14, 16, 18 and 20 interpreted as facies 1a clearly indicate grounded ice not only with S1 and S2 fabrics (Fig. 7) but also due to the presence of cracked grains (Fig. 4A, C) and necking structures (Fig. 4B) formed during homogenisation of the sediment via subglacial deformation. This homogenisation along with the unimodal grain size distribution for core 3R (Orejola et al., 2014) is similar to subglacial tills cored in

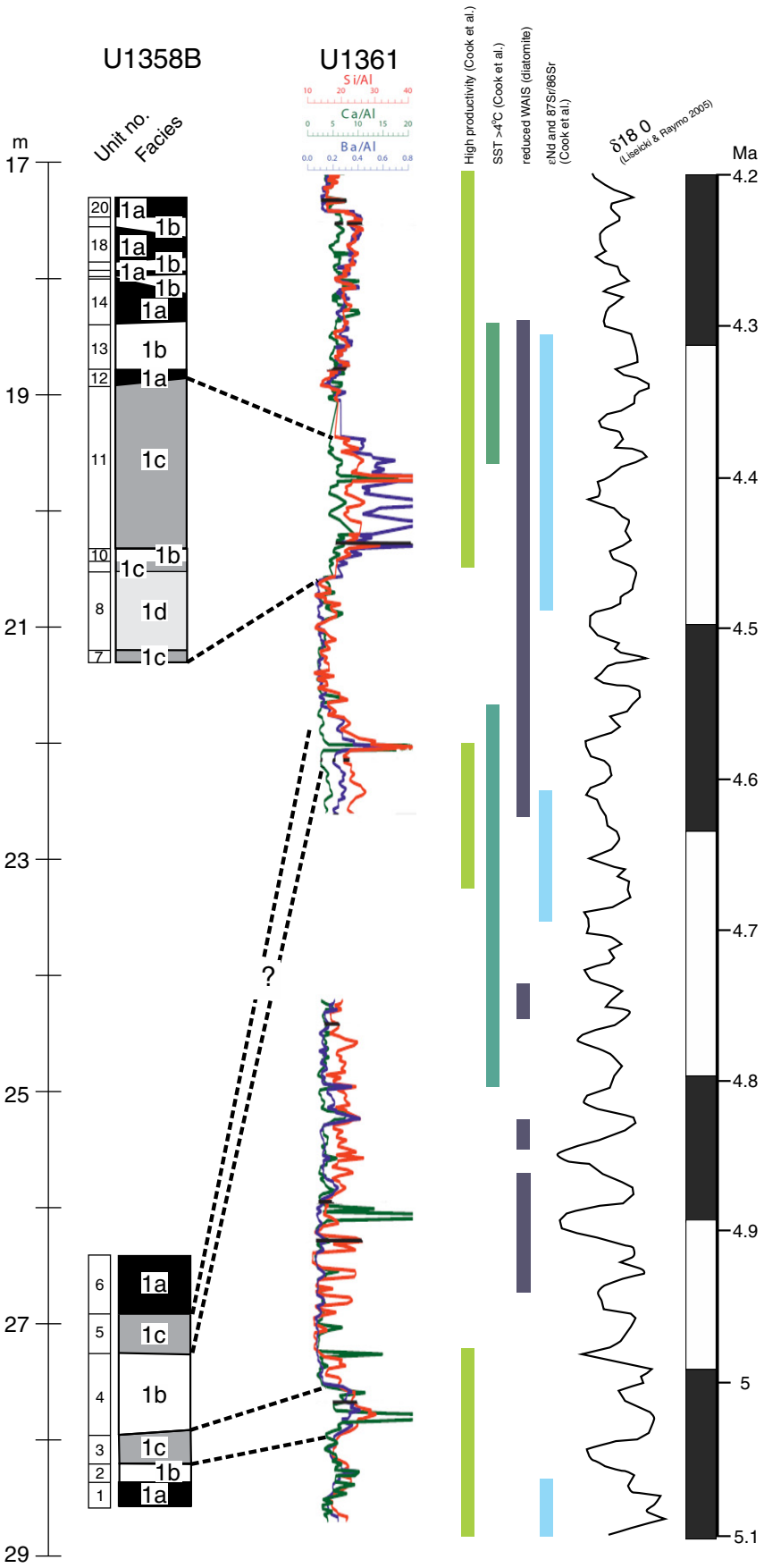
U1358B
U1361
Si/Al
Ca/Al
Ba/Al
Unit no.
Facies
m
17
19
21
23
25
27
29
1a
1b
1c
1d
?
High productivity (Cook et al.)
SST >4°C (Cook et al.)
reduced WAIS (diatomite)
εNd and 87Sr/86Sr (Cook et al.)
δ18 O (Lisiecki & Raymo 2005)
Ma
4.2
4.3
4.4
4.5
4.6
4.7
4.8
4.9
5
5.1

the Ross Sea (Anderson et al., 1980; Mosola and Anderson, 2006; McKay et al., 2009). In units 13, 15, 17 and 19, haloes (Fig. 5B) as well as other varying types of rotation structures (Fig. 5A), pressure shadows (Fig. 5C), and water escape structures (Fig. 5D) are all present and these units were interpreted as facies 1b (Table 1).

Open marine conditions may well have occurred between each advance and retreat phase as indicated from the neighbouring Site U1361 on the continental rise where significantly warmer conditions occurred from 4.2 to 4.4 Ma at the beginning of the *T. innura* zone (Cook et al., 2013), but reworking by grounded ice seems to have removed this from the stratigraphic record in core section 3R-1.

5.6. Diatom analyses

No significant changes of diatom abundance and assemblage have been observed in our samples between the different glacimarine and subglacial units. This is not surprising since grounded ice will rework the underlying marine or glacimarine sediments and therefore the ability to interpret changes in environmental conditions downcore is limited. This assertion is strengthened by the fact that weakly silicified taxa were not observed at U1358; relatively stronger taxa dominate and could explain the low diatom abundance throughout cores 3R and 4R. Even the rare occurrence of open marine diatoms in samples at U1358 may have simply been eroded from interglacial sediments at more coastal locations and transported by grounded ice out onto the shelf as they are found within both glacimarine and subglacial sediments recovered at Site U1358. The process of subglacial transport may be one reason for the poor preservation but if the "open marine" diatoms were deposited "in situ" in open water conditions then selected dissolution or physical destruction could have occurred after deposition to explain the poorly preserved assemblage. It should be noted however that the low preservation of diatom assemblages in open marine units was based on a qualitative analysis of 5 smear slides (Fig. 2) and a more detailed study is currently being prepared to produce a more reliable estimation of diatom concentration (Iwai et al., 2014).

Diatom assemblages suggest that all diatoms found in the samples analysed can be placed into Subzone B of the *T. innura* Zone of the lower Pliocene that ranges from 4.2 to 5.12 Ma. Top and bottom of this subzone are defined by the first occurrence (FO) of *Fragiraliopsis barronii* (4.40 Ma, Cody et al., 2008; Iwai and Kobayashi, unpublished data from Site U1361) and the FO/first common occurrence (FCO) of *Thalassiosira complicata* (5.12 Ma, Winter and Iwai, 2002; Iwai and Kobayashi, unpublished data from Site U1361). Thus, all 10 samples from core sections 3R-1 through 4R-CC are biostratigraphically equivalent to those from Package 2 on the Antarctic Peninsula (Bart and Iwai, 2012). The early Pliocene age confirms previous interpretations made by Escutia et al. (2011) and Orejola et al. (2014).

Diatoms at Site U1358 are not indicative of the sea ice conditions because sea ice diatoms generally have weakly silicified frustules and may be destroyed during deposition, recycling and compaction processes. Only very low concentrations of these species of diatom remain such as *Eucampia antarctica*. Species such as *Rhizosolenia* spp.; *Shionodicus oestrupii*; *Thalassionema nitzschiode* and *Thalassiothrix antarctica* represent a range of conditions from ice-tolerant open ocean species to warmer ocean species. *Shionodiscus oestrupii* and *T. nitzschiodes* have been linked to warm open ocean conditions in the modern Southern Ocean and North Atlantic and to warmer-than-present Pliocene conditions in the Ross Sea and Prydz Bay and the neighbouring Site U1361 (Cook et al., 2013 and the references therein).

Overall, the diatom assemblage at Site U1358 is very similar to that found in the Pliocene section of Site U1361 (although concentrations are much lower at Site U1358). For Site U1361, Cook et al. (2013) note that several extant diatom species with well-constrained modern ecological preferences indicate a high productivity environment with minimal summer/spring sea ice, and warmer-than-present ocean temperatures throughout the Pliocene. They continue that superimposed upon a baseline of warmer-than-present temperatures are intervals of high primary productivity recorded by the presence of diatom-rich sediments and that the significant differences between Pliocene and modern diatom assemblages at Site U1361 demonstrate major differences in environmental conditions during the Pliocene relative to today, most likely associated with warmer sea surface temperatures.

6. Discussion

6.1. Correlation of depositional events to other Antarctic records

Cores 3R and 4R span an age range from 4.2 to 5.12 Ma (Fig. 3). This age model can be refined by comparing results to the neighbouring continental rise Site U1361 (Fig. 9). Peaks in Si/Al, Ca/Al and Ba/Al ratios at U1361 all indicate high ocean productivity (Cook et al., 2013). A distinct prolonged peak in all three ratios occurs between 4.45 and 4.38 Ma and likely corresponds with the prolonged open marine conditions represented by units 7 to 11. It is during this peak at Site U1361 that Cook et al. (2013) suggest retreat of the ice margin several hundred kilometres inland of the current coastline based on the provenance of fine-grained detrital sediments. Several other Antarctic sites also indicate ice retreat. In Prydz Bay, the Sørsdal Formation was deposited in a coastal embayment in <25 m of water between 4.1 and 4.5 Ma (Harwood et al., 2000). During this time, SST were >1.6 °C warmer than today and the presence of aeolian material indicates that the ice-sheet margin was at least 50 km inland of its current position (McKelvey et al., 2001). At ODP Site 1165 there is an increase in dictyocha indicating SST in excess of 5 °C warmer than present between 4.3 and 4.4 Ma (Whitehead and Bohaty, 2003) and summer SST > 5 °C around 4 Ma (Escutia et al., 2009). At the AND-B site a thick (90 m) diatomite layer at around 4.4 Ma indicates open water conditions and the models suggest a collapse of the WAIS (Naish et al., 2009; Pollard and DeConto, 2009).

Based on the correlation of units 7 to 11 with the pronounced peak in warming at Site U1361, the grounded ice events represented in units 13 to 20 would then be younger than 4.38 Ma (Fig. 9). There is not much evidence for cooler conditions around this time although ODP Site 1097 on the Antarctic Peninsula contained subglacial deposits extending throughout the later part of the *T. innura* timespan (Bart and Iwai, 2012).

Core 4R has two distinct units (3 and 5) that were deposited in open marine conditions and these units are correlated to two distinct warm events at Site U1361 (Fig. 9). The first probably took place at approximately 4.58 Ma which also correlates to diatomite layers from AND-1B indicating warm open water conditions but it could also relate to a smaller warm event around 4.88 Ma. The second period of open marine conditions took place between 5.05 and 5 Ma, which also correlates to a period of high productivity at Site U1361. Thus there must have been an advance of ice represented by unit 6 between about 4.58 and 4.45 Ma. Earlier ice advance between the two warm peaks (unit 4) correlates with cooler conditions at Prydz Bay around 4.95 to 5 Ma but is not long lasting as warm condition prevails by 5 Ma at Site U1361. There

Fig. 9. Correlation of the depositional events interpreted from U1358 with the neighbouring rise Site U1361. The dashed lines correlate open marine conditions at U1358 to periods with increased ratios of εNd and $^{87}Sr/^{86}Sr$ (light blue bars) characteristic of sediments deposited during periods of Pliocene warmth and Si/Al; Ca/Al and Ba/Al with higher productivity at U1361 as outlined by Cook et al. (2013). Also included is the magnetostratigraphic control used by Cook et al. (2013). Periods of warmer SST set out by Bohaty and Harwood (1998) and Escutia et al. (2009) are also included (light and dark green bars). Dark blue bars indicate periods when WAIS is thought to have collapsed and diatomite layers were deposited at the AND-1B site (McKay et al., 2009) and the global $\delta^{18}O$ curve of Lisiecki and Raymo (2005).

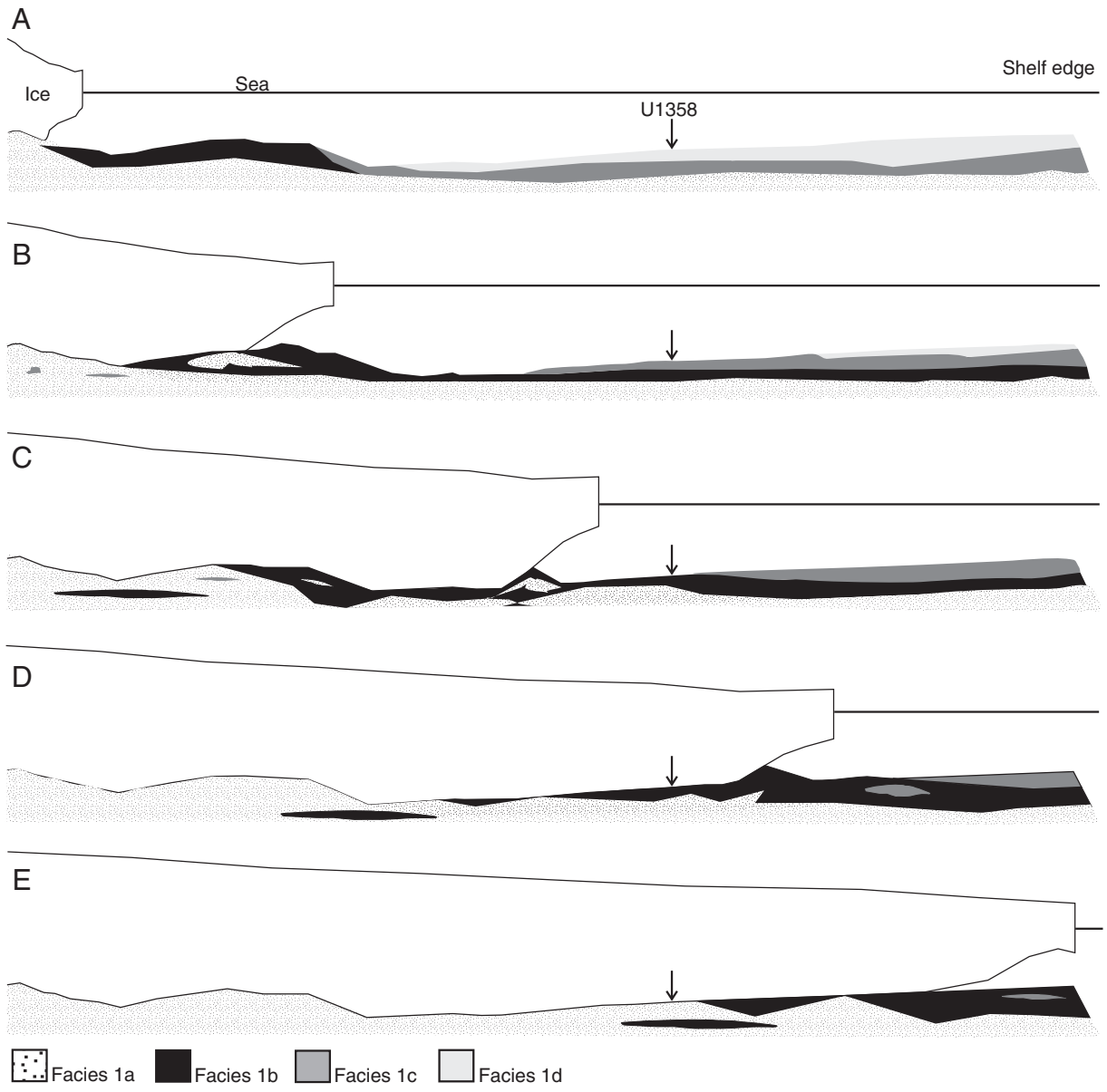

Fig. 10. A to E) Schematic diagram of the facies type deposited at Site U1358 (indicated by arrow) during one grounded ice advance from the inner shelf to the outer shelf (see text for explanation).

does not seem to be any clear correlation with the stratigraphically oldest ice advance (unit 1) which must have occurred before 5.05 Ma.

It is not possible to interpret the length of transition from grounded ice to open marine conditions and vice versa and if these transitions were all of similar length. However, proxies from U1361 indicate that peaks in productivity and SST happened relatively rapidly (Cook et al., 2013) so it is probable that the transition from grounded ice to open marine conditions could have occurred relatively rapidly too. At the AND-1B site the transition from till (subglacial) to diatomite (open marine) can sometimes be represented by only 1 m of material (McKay et al., 2009) thus preservation of such transitional units at Site U1358 may be negligible.

This study shows for the first time direct evidence of both open marine and grounded ice conditions on the shelf offshore from the Wilkes Subglacial Basin during the early Pliocene (between 4.2 and 5.12 Ma). Our study confirms previous interpretations from the neighbouring rise Site U1361, suggesting a dynamic EAIS with the ice margin repeatedly retreating and advancing during this period. From seismic data, Bart (2001) had previously suggested at least one advance of the EAIS to the outer shelf in Prydz Bay during the early Pliocene and Bart and Iwai (2012) note that there were at least nine outer shelf grounding events of the Antarctic Peninsula Ice Sheet during the *T. innura* sub-zone B time frame. The preserved record shows that Antarctic Peninsula Ice Sheet advances in the preceding *T. innura* sub-zone A were even more frequent. It is very probable that not all the advances and retreats of the grounding line between 4.2 and 5.12 Ma have been preserved within cores 3R and 4R but our results do indicate dynamic ice sheet behaviour throughout the period. It is not surprising that more grounded/ice proximal units were recovered in comparison to open marine/ice distal units, this simply relates to lower preservation potential of interglacial deposits on the shelf during successive glacial advances. Even the most recent interglacial is sometimes not recovered from the shelf (Escutia et al., 2003).

In contrast to the initial studies of Site U1358, this study shows at least four distinct grounding line advances and three periods when the grounding line was distal to Site U1358 (Fig. 9). Similar fluctuations in SST proxies and supply of terrigenous material within the early Pliocene are observed from cores from the Wilkes Land continental

rise at Site U1361, Prydz Bay, AND-1B and the Antarctic Peninsula suggesting that it is less likely that facies 1a and 1b represent just localised ice advance in the form of palaeo-ice streams advancing within cross-shelf troughs to the shelf edge.

6.2. Significance of laminated units

Units 3, 5, 7 to 9 and 11 are all laminated or partially laminated (Figs. 2 and 8). There are several mechanisms by which the laminae may have formed in an open marine shelf environment. Recent studies have shown that it is even possible for subglacial sediment to contain laminae relating to pressurised water flow (Phillips et al., 2012) but the supporting micromorphological data all indicate deposition in an open marine environment. In particular, the laminae are preserved even at a micro-scale (Fig. 6B). The laminated sequences lack the grading, sharp contacts and rhythmic nature of laminated units deposited ice proximally (Ó Cofaigh and Dowdeswell, 2001). They also lack microstructures such as sheath folds, augen-shapes, normal faults, reverse/thrust faults, partially destroyed clasts, dropstones and realigned bedding that would indicate significant modification by iceberg scouring (Linch, 2010; Linch et al., 2012) although some localised shears indicated by grain lineations were present but are probably post-depositional. There is also a lack of evidence of heterogeneous coarser grained material in facies 1c and 1d that would be expected with significant iceberg rafting in a proximal grounding line environment. It should be noted that while Orejola et al. (2014) did not interpret the laminae as a primary glacitectonic features we suggest that the apparent dip of the laminae is a post-depositional glacitectonic effect rather than caused by iceberg scouring as they suggest. Some of the larger clasts in facies 1c and 1d are clearly ice-rafted debris but sand enrichment and sorting in core 4R would suggest that deposition is mainly dependent on winnowing from currents rather than ice-rafted supply (Denis et al., 2009; Orejola et al., 2014). Cook et al. (2013) also noted that for the neighbouring Site U1361 some post-depositional winnowing of fine-grained sediment components during warmer intervals may have taken place. The laminated units are interpreted as mainly relating to ocean current processes but may also contain small amounts of ice-rafted material with limited iceberg scouring which would have further disrupted the fine laminae (Domack, 1982, 1988; McMullen et al., 2006).

6.3. Dynamics of the grounding line

The identification and interpretation of the depositional process that produced the different facies observed within cores 3R and 4R provide the first evidence of grounded ice migration on this part of the East Antarctic margin. When the grounding line was situated on the inner shelf or landward of the inner shelf, deposition of the laminated facies 1d would have occurred at Site U1358 (Fig. 10A). When the grounding line started advancing onto the shelf, these laminated units would become partially disrupted with a comparatively higher energy depositional environment at U1358 including deposition of coarser material some of which may have been ice-rafted or transported via meltwater plumes. During this period facies 1c would be deposited at U1358 (Fig. 10B). As the grounding line continued to advance onto the outer shelf, facies 1b would have been deposited at U1358 with grounding line proximal processes such as reworking of till and debris flows occurring (Fig. 10C) but also the initiation of subglacial deformation as grounded ice passed over the site (Fig. 10D). With the grounding line situated on the outer shelf, sediments would have undergone significant homogenisation within a deforming continuum represented by facies 1a at U1358 (Fig. 10E). The same process in reverse could have taken place as the grounding line retreated back across the shelf.

A major question that still remains is how far inland did the grounding line retreat during periods of open marine conditions at Site U1358 (Fig. 10A). It is suggested that the grounding line would have had to be at least as distal as it is today, i.e. along the present coast line to allow the suspension settling of the fine grained sediments, however it may have retreated much further inland. Cook et al. (2013) note that a lack of geological and geophysical data in the region connecting the coastal areas at the mouth of the Wilkes Subglacial Basin with the main central inland part of the basin inhibits a precise estimate on how far the ice margin may have retreated inland. Certainly the area of the present day coast line is elevated in comparison to both on-shore and off-shore basins and would act as a natural pinning point for the grounding line (Fig. 1) (e.g. Greenwood et al., 2012). However, Mengel and Levermann's (2014) ice sheet model suggests that with removal of this coastal ice or "ice plug" would lead to rapid discharge of ice from the entire Wilkes Basin. Based on their provenance study, Cook et al. (2013) believe that the ice must have retreated into the central portion of the Wilkes Subglacial Basin. It is interesting to note that conversely, based on one sample taken from core section 3R1 when the grounding line was on the outer shelf, neodymium isotopic provenance indicates that sediments were supplied from the Adèlie Craton i.e. the coastal area rather than the Wilkes Subglacial Basin which may have only been the source of the sediment as the grounding line retreated back towards the inner shelf (Cook, unpublished data).

One important factor that may have varied in early Pliocene times compared to later ice advances and retreats during the Pleistocene is the basal thermal regime. Palaeo-ice streams flowing though cross-shelf troughs will have always been warm-based but inter-ice stream areas such as the Mertz Bank were almost certainly overlain by cold-based ice or at very least slow moving ice during cold polar conditions such as the LGM (Eittreim et al., 1995; Reinardy et al., 2011a,b; Klages et al., 2013). The circular depressions described by Barnes (1987) on the Mertz Bank are probably hill–hole pairs that document slow flow of cold-based ice during the LGM, strongly-coupled to its bed (Klages et al., 2013). Regionally, this may have stabilised the grounding line to some extent (Joughin et al., 2003; Whillans and van der Veen, 2001; Whillans et al., 2001; Presti et al., 2005; van der Veen et al., 2007). With the elevated SST of the early Pliocene these inter-stream ridges, which may have migrated over time (Eittreim et al., 1995; Escutia et al., 2003), along with the grounding line, may have been far less stable (cf. Jenkins et al., 2010) allowing considerable retreat of ice inland as suggested by Cook et al. (2013).

The data presented here provide conclusive evidence for ice retreat and advance and hence support the interpretations made from the rise site as well as from ice sheet models. Thus, it is now possible to show that the EAIS was a dynamic ice sheet during the early Pliocene that was probably far more sensitive to climatic and oceanic forcing even during relatively short time periods than had previously been thought. It also has important implications for the future behaviour and sensitivity of the EAIS under present continuing warming conditions.

7. Conclusions

The analysis of the diatom assemblage from Site U1358 has greatly improved the chronological framework of the lower part of core 1358B section 3R and 4R. The assemblage dated back to the *T. innura* Zone of the lower Pliocene that ranges from 4.2 to 5.12 Ma. Based on the identification and interpretation of four facies types, this study correlates the three periods of prolonged open marine conditions represented by the laminated facies 1c and 1d with periods of elevated productivity and sea surface temperatures from the neighbouring rise Site U1361. Between these periods of open marine conditions on the shelf, grounded ice extended to the shelf edge represented by facies 1a and 1b which both contain evidence of subglacial deformation. It appears that grounded ice advanced onto the shelf around 5.1 Ma (Fig. 9). The longevity of this event is unclear as it forms the lowermost unit in core section 4R-CC and may extend back to earlier times. Following this there was open marine conditions at around 5.05 to 5 Ma followed by an ice advance at between 5 and 4.58 Ma. A second period of open

marine conditions occurred around 4.58 Ma with grounded ice returning relatively soon after this but definitely before 4.45 Ma. A prolonged period of open marine conditions then persisted from 4.45 to 4.38 Ma. Assuming that the top of core 3R-1 represents the beginning of Subzone B of *T. innura* then ice proximal conditions dominated from 4.38 to 4.2 Ma. Thus, this study shows that proxies from the deep ocean and continental rise used to indicate a dynamic ice sheet with advance and retreat of the grounding line can also be linked with the direct evidence of these fluctuations from the shelf. Together, this evidence provides important constraints on new ice sheet models from the region.

Acknowledgements

This research used samples and data provided by the Integrated Ocean Drilling Program (IODP). The IODP is sponsored by the US National Science Foundation (NSF) and participating countries under the management of the Joint Oceanographic Institutions. Financial support for this study was provided by the Spanish Ministry of Science and Innovation grant CTM 2011-24079 and ERA-NET European Partnership in Polar Climate Science (EUROPOLAR) — EUI2009-04040. We would also like to thank Adrian Palmer for a great deal of help and assistance with the preparation and production of thin sections as well as helpful discussions with Johann Klages, Emrys Phillips and Sandra Passchier. We thank Philip Bart and an anonymous reviewer for their helpful reviews that improved this manuscript.

References

Anderson, J.B., Kurtz, D.D., Domack, E.W., Balshaw, K.K., 1980. Glacial and glacial marine sediments of the Antarctic continental shelf. J. Geol. 88, 399–414.
Barnes, P.W., 1987. Morphological studies of the Wilkes Land continental shelf, Antarctica — glacial and iceberg effects. In: Eittreim, S.L., Hampton, M.A. (Eds.), The Antarctic Continental Margin Geology and Geophysics of Offshore Wilkes Land. CPCEMR EARTH Science Series, Circum-Pacific Council for Energy and Mineral Resources, Houston, pp. 75–88.
Barnes, P.W., Lien, R., 1988. Icebergs rework shelf sediments to 500 m off Antarctica. Geology 16, 1130–1133.
Baroni, C., Fasano, F., 2006. Micromorphological evidence of warm-based glacier deposition from the Ricker Hills Tillite (Victoria Land, Antarctica). Quat. Sci. Rev. 25, 976–992.
Barker, P.F., Barrett, P.J., Cooper, A.K., Huybrechts, P., 1999. Antarctic glacial history from numerical models and continental margin sediments. Palaeogeogr. Palaeoclimatol. Palaeoecol. 150, 247–267.
Bart, P.J., 2001. Did the Antarctic ice sheets expand during the early Pliocene? Geology 29, 67–70.
Bart, P.J., Iwai, M., 2012. The overdeepening hypothesis: how erosional modification of the marine-scape during the early Pliocene altered glacial dynamics on the Antarctic Peninsula's Pacific margin. Palaeogeogr. Palaeoclimatol. Palaeoecol. 335, 42–51.
Bart, P.J., De Batist, M., Jokat, W., 1999. Interglacial collapse of Crary trough-mouth fan, Weddell Sea, Antarctica: implications for Antarctic glacial history. J. Sediment. Res. 69, 1276–1289.
Bart, P.J., Hillenbrand, C.-D., Ehrmann, W., Iwai, M., Winter, D., Warny, S.A., 2007. Are Antarctic Peninsula Ice Sheet grounding events manifest in sedimentary cycles on the adjacent continental rise? Mar. Geol. 236, 1–13.
Beaman, R.J., O'Brien, P.E., Post, A.L., De Santis, L., 2010. A new high-resolution bathymetry model for the Terre Adélie and George V continental margin, East Antarctica. Antarct. Sci. 23, 95–103.
Bohaty, S.M., Harwood, D.M., 1998. Southern Ocean Pliocene paleotemperature variation from high-resolution silicoflagellate biostratigraphy. Mar. Micropaleontol. 33, 241–272.
Bælum, K., Benn, D.I., 2011. Thermal structure and drainage system of a small valley glacier (Tellbreen, Svalbard), investigated by ground penetrating radar. Cryosphere 5, 139–149.
Carr, S.J., 1999. The micromorphology of Last Glacial Maximum sediments in the Southern North Sea. Catena 35, 123–145.
Carr, S.J., 2001. Micromorphological criteria for discriminating subglacial and glacimarine sediments: evidence from a contemporary tidewater glacier, Spitsbergen. Quatern. Int. 86, 71–79.
Carr, S.J., Rose, J., 2003. Till fabric patterns and significance: particle response to subglacial stress. Quatern. Sci. Rev. 22, 1415–1426.
Carr, S.J., Holmes, R., van der Meer, J.J.M., Rose, J., 2006. The Last Glacial Maximum in the North Sea Basin: micromorphological evidence of extensive glaciation. J. Quatern. Sci. 21, 131–153.
Chaolu, Y., Zhijiu, C., 2001. Subglacial deformation: evidence from microfabric studies of particles and voids in till from the upper Ürümqi river valley, Tien Shan, China. J. Glaciol. 47, 607–612.
Cody, R.D., Levy, R.H., Harwood, D.M., Sadler, P.M., 2008. Thinking outside the zone: high-resolution quantitative diatom biochronology for the Antarctic Neogene. Palaeogeogr. Palaeoclimatol. Palaeoecol. 260, 92–121.
Cook, C.P., van de Flierdt, T., Williams, T., Hemming, S.R., Iwai, M., Kobayashi, M., Jimenez-Espejo, F.J., Escutia, C., González, J.J., Khim, B., McKay, R.M., Passchier, S., Bohaty, S.M., Riesselman, C.R., Tauxe, L., Sugisaki, S., Galindo, A.L., Patterson, M., Sangiorgi, F., Pierce, E.L., Brinkhuis, H., IODP Expedition 318 Scientists, 2013. Dynamic behaviour of the East Antarctic Ice Sheet during Pliocene warmth. Nat. Geosci. 6, 765–769.
Cooper, A.K., Brancolini, G., Escutia, C., Kristoffersen, Y., Larter, R., Leitchenkov, G., O'Brien, P., Jokat, W., 2009. Cenozoic climate history from seismic-reflection and drilling studies on the Antarctic continental margin. In: Florindo, F., Siegert, M. (Eds.), Antarctic Climate Evolution. Developments in Earth and Environmental Sciences, No. 8. Elsevier, Amsterdam, pp. 115–228.
DeConto, R.M., Pollard, D., 2003. A coupled climate–ice sheet modeling approach to the early Cenozoic history of the Antarctic ice sheet. Palaeogeogr. Palaeoclimatol. Palaeoecol. 198, 39–52.
Denis, D., Crosta, X., Schmidt, S., Carson, D., Ganeshram, R., Renssen, H., Bout-Roumazeilles, V., Zaragosi, S., Martin, B., Giraudeau, J., 2009. Glacier and deep water Holocene dynamics, Adélie Land region, East Antarctica. Quatern. Sci. Rev. 28, 1291–1303.
De Santis, L., Brancolini, G., Donda, F., 2003. Seismic-stratigraphic analysis of the Wilkes Land continental margin (East Antarctica). Influence of glacially-driven processes on the Cenozoic deposition. Deep-Sea Res. 50, 1563–1594.
Dolan, A.M., Haywood, A.M., Hill, D.J., Dowsett, H.J., Hunter, S.J., Lunt, D.J., Pickering, S.J., 2011. Sensitivity of Pliocene ice sheets to orbital forcing. Palaeogeogr. Palaeoclimatol. Palaeoecol. 309, 98–110.
Domack, E.W., 1982. Sedimentology of glacial and glacial marine deposits in the George V-Adelie continental shelf, East Antarctica. Boreas 11, 79–98.
Domack, E.W., 1988. Biogenic facies in the Antarctic glaciomarine environment: basis for a polar glacimarine summary. Palaeogeogr. Palaeoclimatol. Palaeoecol. 63, 357–372.
Ehlers, J., Gibbard, G.L., Whiteman, C.A., 1987. Recent investigations of the Marly Drift of northernwest Norfolk, England. In: van der Meer, J.J.M. (Ed.), Tills and Glaciotectonics. Balkema, Rotterdam, pp. 39–54.
Eittreim, S.L., Cooper, A.K., Wannesson, J., 1995. Seismic stratigraphic evidence of ice-sheet advances on the Wilkes Land margin of Antarctica. Sediment. Geol. 96, 131–156.
Escutia, C., Eittreim, S.L., Cooper, A.K., 1997. Cenozoic glaciomarine sequences on the Wilkes Land continental rise. Antarctica: Proceedings Vol. VII. International Symposium on Antarctic Earth Sciences, pp. 791–795.
Escutia, C., Warnke, D.A., Acton, G.D., Barcena, A., Burckle, L., Canals, M., Frazee, C.S., 2003. Sediment distribution and sedimentary processes across the Antarctic Wilkes Land margin during the Quaternary. Deep-Sea Res. Part 2. Topical Stud. Oceanogr. 50, 1481–1508.
Escutia, C., De Santis, L., Donda, F., Dunbar, R.B., Cooper, A.K., Brancolini, G., Eittreim, S.L., 2005. Cenozoic ice sheet history from East Antarctic Wilkes Land continental margin sediments. Global Planet. Chang. 45, 51–81.
Escutia, C., Bárcena, M.A., Lucchi, R.G., Romero, O., Ballegeer, A.M., Gonzalez, J.J., Harwood, D.M., 2009. Circum-Antarctic warming events between 4 and 3.5 Ma recorded in marine sediments from the Prydz Bay (ODP Leg 188) and the Antarctic Peninsula (ODP Leg 178) margins. Global Planet. Chang. 69, 170–184.
Escutia, C., Brinkhuis, H., Klaus, A., Expedition 318 Scientists, 2011. Proceeding of the Integrated Ocean Drilling Program, Expedition 318. Integrated Ocean Drilling Program Management International, College Station, TX http://dx.doi.org/10.2204/iodp.proc.318.101.2011.
Evans, J., Pudsey, C.J., Ó Cofaigh, C., Morris, P., Domack, E., 2005. Late Quaternary glacial history, flow dynamics and sedimentation along the eastern margin of the Antarctic Peninsula Ice Sheet. Quatern. Sci. Rev. 24, 741–774.
Greenwood, S.L., Gyllencreutz, R., Jakobsson, M., Anderson, J.B., 2012. Ice-flow switching and East/West Antarctic Ice Sheet roles in glaciation of the western Ross Sea. Geol. Soc. Am. Bull. 124, 1736–1749.
Harris, P.T., Brancolini, G., Armand, L., Busetti, M., Beaman, R.J., Giorgetti, G., Presti, M., Trincardi, F., 2001. Continental shelf drift deposit indicates non-steady state Antarctic Bottom Water production in the Holocene. Mar. Geol. 179, 1–8.
Harwood, D.M., McMinn, A., Quilty, P.G., 2000. Diatom biostratigraphy and age of the Pliocene Sørsdal Formation, Vestfold Hills, East Antarctica. Antarct. Sci. 12, 443–462.
Haywood, A.M., Hill, D.J., Dolan, A.M., Otto-Bliesner, B.L., Bragg, F., Chan, W.-L., Chandler, M.A., Contoux, C., Dowsett, H.J., Jost, A., Kamae, Y., Lohmann, G., Lunt, D.J., Abe-Ouchi, A., Pickering, S.J., Ramstein, G., Rosenbloom, N.A., Salzmann, U., Sohl, L., Stepanek, C., Ueda, H., Yan, Q., Zhang, Z., 2012. Large-scale features of Pliocene climate: results from the Pliocene Model Intercomparison Project. Clim. Past Discuss. 9, 191–209.
Hicock, S.R., Goff, J.R., Lian, O.B., Little, E.C., 1996. On the interpretation of subglacial till fabric. J. Sediment. Res. 66, 928–934.
Hiemstra, J.F., 1999. Microscopic evidence of grounded ice in the sediments of the CIROS-1 Core, McMurdo Sound, Antarctica. Terra Antarct. 6, 365–376.
Hiemstra, J.F., van der Meer, J.J.M., 1997. Pore-water controlled grain fracturing as an indicator for subglacial shearing in tills. J. Glaciol. 43, 446–454.
Hiemstra, J.F., Zaniewski, K., Powell, R.D., Cowan, E.A., 2004. Strain signatures of fjord sediment sliding: micro-scale examples from Yakutat Bay and Glacier Bay, Alaska, U.S.A. J. Sediment. Petrol. 76, 760–769.
Hill, D.J., Haywood, A.M., Hindmarsh, R.C.M., Valdes, P.J., 2007. Characterizing ice sheets during the Pliocene: evidence from data and models. In: Williams, M., Haywood, A.M., Gregory, J., Schmidt, D.N. (Eds.), Deep-Time Perspectives on Climate Change: Marrying the Signal From Computer Models and Biological Proxies. Micropalaeontological Society Special Publication, Geological Society of London, pp. 517–538.

Huybrechts, P., 1994. Formation and disintegration of the Antarctic ice sheet. Ann. Glaciol. 20, 336–340.
IPCC (Intergovernmental Panel on Climate Change), 2013. Climate Change 2013: the physical science basis. Contribution of Working Group I to the 5th Assessment Report of the Intergovernmental Panel on Climate Change. Cambridge University Press, Cambridge.
Iwai, M., Reinardy, B.T.I., Escutia, C., IODP Expedition 318 Scientists, 2014. Diatom age assignment at IODP Site U1358 on the continental shelf off the Adelie Coast, Antarctica. EGU General Assembly 2014, Vienna, Austria, 9804.
Jenkins, A., Dutrieux, P., Jacobs, S.S., McPhail, S.D., Perrett, J.R., Webb, A.T., White, D., 2010. Observations beneath Pine Island Glacier in West Antarctica and implications for its retreat. Nat. Geosci. 3, 468–472.
Joughin, I., Rignot, E., Rosanova, C.E., Lucchitta, B.K., Bohlander, J., 2003. Timing of recent accelerations of Pine Island Glacier, Antarctica. Geophys. Res. Lett. 30. http://dx.doi.org/10.1029/2003GL017609.
Kalvāns, A., Saks, T., 2008. Two-dimensional apparent microfabric of the basal Late Weichselian till and associated shear zone: case study from western Latvia. Estonian J. Earth Sci. 57, 241–255.
Kilfeather, A., Ó Cofaigh, C., Dowdeswell, J.A., van der Meer, J.M., Evans, D.J., 2010. Micromorphological characteristics of glacimarine sediments: implications for distinguishing genetic processes of massive diamicts. Geo-Mar. Lett. 30, 77–97.
Klages, J.P., Kuhn, G., Hillenbrand, C.-D., Graham, A.G.C., Smith, J.A., Larter, R.D., Gohl, K., 2013. First geomorphological record and glacial history of an inter-ice stream ridge on the West Antarctic continental shelf. Quatern. Sci. Rev. 61, 47–61.
Larsen, N.K., Piotrowski, J.A., Menzies, J., 2007. Microstructural evidence of low strain, time-transgressive subglacial deformation. J. Quatern. Sci. 22, 593–608.
Lea, J.M., Palmer, A., 2014. Quantification of turbate microstructures through a subglacial till: dimensions and characteristics. Boreas 43, 869–881.
Lee, J.R., Phillips, E., 2013. Glacitectonics — a key approach to examining ice dynamics, substrate rheology and ice-bed coupling. Proc. Geol. Assoc. 124, 731–737.
Licht, K.J., Dunbar, N.W., Andrews, J.T., Jennings, A.E., 1999. Distinguishing subglacial till and glacial marine diamictons in the western Ross Sea, Antarctica: implications for a last glacial maximum grounding line. Geol. Soc. Am. Bull. 111, 91–103.
Linch, L.D., 2010. Micromorphology of Iceberg Scour. (Ph.D. thesis). Queen Mary University of London, London.
Linch, L.D., van der Meer, J.J.M., Menzies, J., 2012. Micromorphology of iceberg scour in clays: Glacial Lake Agassiz, Manitoba, Canada. Quatern. Sci. Rev. 55, 125–144.
Lisiecki, L.E., Raymo, M.E., 2005. A Pliocene–Pleistocene stack of 57 globally distributed benthic d18O records. Paleoceanography 20. http://dx.doi.org/10.1029/2004PA001071.
Lowe, A.S., Anderson, J.B., 2002. Reconstruction of the West Antarctic ice sheet in Pine Island Bay during the Last Glacial Maximum and its subsequent retreat history. Quatern. Sci. Rev. 21, 1879–1897.
McKay, R.M., Browne, G.H., Carter, L., Cowan, E.A., Dunbar, G.B., Krissek, L.A., Naish, T.R., Powell, R.D., Reed, J.A., Wilch, T.I., 2009. The stratigraphic signature of late Cenozoic oscillations of the West Antarctic Ice Sheet in Ross Embayment. Geol. Soc. Am. Bull. 121, 1537–1561.
McKelvey, B., Hambrey, M., Harwood, D., Mabin, M., Webb, P., Whitehead, J., 2001. The Pagodroma Group: the Neogene record in the northern Prince Charles Mountains of a dynamic Lambert Glacier and East Antarctic Ice Sheet. Antarct. Sci. 13, 455–468.
McMullen, K., Domack, E., Leventer, A., Olson, C., Dunbar, R.B., Brachfeld, S., 2006. Glacial morphology and sediment formation in the Mertz Trough, East Antarctica. Palaeogeogr. Palaeoclimatol. Palaeoecol. 231, 169–180.
Mengel, M., Levermann, A., 2014. Ice plug prevents irreversible discharge from east Antarctica. Nat. Clim. Chang. 4, 451–455.
Menzies, J., 2000. Micromorphological analyses of microfabrics and microstructures indicative of deformation processes in glacial sediments. In: Maltman, A.J., Hubbard, B., Hambrey, M.J. (Eds.), Deformation of Glacial Materials. Geological Society Special Publication, London, pp. 245–257.
Miller, K.G., Wright, J.D., Browning, J.V., Kulpecz, A., Kominz, M., Naish, T.R., Cramer, B.S., Rosenthal, Y., Peltier, R., Sosdian, S., 2012. High tide of the warm Pliocene: implications of global sea level for Antarctic deglaciation. Geology 40, 407–410.
Mosola, A.B., Anderson, J.B., 2006. Expansion and rapid retreat of the West Antarctic Ice Sheet in eastern Ross Sea: possible consequence of over-extended ice streams? Quatern. Sci. Rev. 25, 2177–2196.
Naish, T., Powell, R., Levy, R., Wilson, G., Scherer, R., Talarico, F., Krissek, L., Niessen, F., Pompilio, M., Wilson, T., Carter, L., DeConto, R.M., Huybers, P., McKay, R., Pollard, D., Ross, J., Winter, D., Barrett, P., Browne, G., Cody, R., Cowan, E., Crampton, J., Dunbar, G., Dunbar, N., Florindo, F., Gebhardt, C., Graham, I., Hannah, M., Hansaraj, D., Harwood, D., Helling, D., Henrys, S., Hinnov, L., Kuhn, G., Kyle, P., Laufer, A., Maffioli, P., Magens, D., Mandermack, K., McIntosh, W., Millan, C., Morin, R., Ohneiser, C., Paulsen, T., Persico, D., Raine, I., Reed, J., Riesselman, C., Sagnotti, L., Schmitt, D., Sjunneskog, C., Strong, P., Taviani, M., Vogel, S., Wilch, T., Williams, T., 2009. Obliquity-paced Pliocene West Antarctic ice sheet oscillations. Nature 458, 322–328.
Ó Cofaigh, C., Dowdeswell, J.A., 2001. Laminated sediments in glacimarine environments: diagnostic criteria for their interpretation. Quatern. Sci. Rev. 20, 1411–1436.
Ó Cofaigh, C., Dowdeswell, J.A., Allen, C.S., Hiemstra, J.F., Pudsey, C.J., Evans, J., Evans, D.J.A., 2005. Flow dynamics and till genesis associated with marine based Antarctic palaeo-ice stream. Quatern. Sci. Rev. 24, 709–740.
Oerlemans, J., 1982. Response of the Antarctic Ice Sheet to a climatic warming: a model study. J. Climatol. 2, 1–11.
Orejola, N., Passchier, S., Expedition 318 Scientists, 2014. Sedimentology of Lower Pliocene to Upper Pleistocene diamictons from IODP Site U1358, Wilkes Land margin, and implications for East Antarctic Ice Sheet dynamics. Antarct. Sci. 26, 183–192.
Pagani, M., Liu, Z., LaRiviere, J., Ravelo, A.C., 2010. High Earth-system climate sensitivity determined from Pliocene carbon dioxide concentrations. Nat. Geosci. 3, 27–30.
Palmer, A.P., 2005. The micromorphological Description, Interpretation and Palaeoenvironmental Significance of Lacustrine Clastic Laminated Sediments. (PhD thesis), University of London, London (chapter 3).
Passchier, S., 2000. Soft-sediment deformation features in core from CRP-2/2A, Victoria Land Basin, Antarctica. Terra Antarct. 7, 401–412.
Passchier, S., 2011. Linkages between East Antarctic Ice Sheet extent and Southern Ocean temperatures based on a Pliocene high-resolution record of ice-rafted debris off Prydz Bay, East Antarctica. Paleoceanography 26. http://dx.doi.org/10.1029/2010PA002061.
Phillips, E., 2006. Micromorphology of a debris flow deposit: evidence of basal shearing, hydrofracturing, liquefaction and rotational deformation during emplacement. Quatern. Sci. Rev. 25, 720–738.
Phillips, E.R., van der Meer, J.J.M., Ferguson, A., 2011. A new 'microstructural mapping' methodology for the identification, analysis and interpretation of polyphase deformation within subglacial sediments. Quatern. Sci. Rev. 30, 2570–2596.
Phillips, E., Everest, J., Reeves, H., 2012. Micromorphological evidence for subglacial multiphase sedimentation and deformation during overpressurized fluid flow associated with hydrofracturing. Boreas 42, 395–427.
Pollard, D., DeConto, R.M., 2009. Modelling West Antarctic ice sheet growth and collapse through the past five million years. Nature 458, 329–332.
Powell, R.D., Cooper, J.M., 2002. A glacial sequence stratigraphic model for temperate, glaciated continental shelves. In: Dowdeswell, J., Ó Cofaigh, C. (Eds.), Glacier-influenced Sedimentation on High-latitude Continental Margins. Geological Society, London Special Publications, London, pp. 215–244.
Powell, R.D., Domack, E.W., 2002. Glacimarine environments. In: Menzies, J. (Ed.), Modern and Past Glacial Environments. Butterworth-Heinemann, Boston, pp. 361–390.
Presti, M., De Santis, L., Brancolini, G., Harris, P.T., 2005. Continental shelf record of the East Antarctic Ice Sheet evolution: seismo-stratigraphic evidence from the George V Basin. Quatern. Sci. Rev. 24, 1223–1241.
Pritchard, H., Athern, R., Vaughan, D., Edwards, L., 2009. Extensive dynamic thinning on the margins of the Greenland and Antarctic ice sheets. Nature 461, 971–975.
Rebesco, M., Camerlenghi, A., Geletti, R., Canals, M., 2006. Margin architecture reveals the transition to the modern Antarctic Ice Sheet (AIS) at about 3 Ma. Geology 34, 301–304.
Reinardy, B.T.I., Lukas, S., 2009. The sedimentary signature of ice-contact sedimentation and deformation at macro- and microscale: a case study from NW Scotland. Sediment. Geol. 221, 87–98.
Reinardy, B.T.I., Hiemstra, J., Murray, T., Hillenbrand, C.-D., Larter, R., 2011a. Till genesis at the bed of an Antarctic Peninsula palaeo-ice stream as indicated by micromorphological analysis. Boreas 40, 498–517.
Reinardy, B.T.I., Hillenbrand, C.-D., Murray, T., Larter, R., Hiemstra, J., Booth, A., 2011b. Streaming flow of an Antarctic Peninsula palaeo-ice stream by both basal sliding and deformation. J. Glaciol. 57, 596–608.
Reinardy, B.T.I., Leighton, I., Marx, P.J., 2013. Glacier thermal regime linked to processes of annual moraine formation at Midtdalsbreen, southern Norway. Boreas 42, 896–911.
Roberts, D.H., Hart, J.K., 2005. The deforming bed characteristics of a stratified till assemblage in north East Anglia, UK: investigating controls on sediment rheology and strain signatures. Quatern. Sci. Rev. 24, 123–140.
Shepherd, A., Ivins, E.R., Geruo, A., Barletta, V.R., Bentley, M.J., Bettadpur, S., Briggs, K.H., Bromwich, D.H., Forsberg, R., Galin, N., Horwath, M., Jacobs, S., Joughin, I., King, M.A., Lenaerts, J.T.M., Li, J., Ligtenberg, S.R.M., Luckman, A., Luthcke, S.B., McMillan, M., Meister, R., Milne, G., Mouginot, J., Muir, A., Nicolas, J.P., Paden, J., Payne, A.J., Pritchard, H., Rignot, E., Rott, H., Sandberg Sørensen, L., Scambos, T.A., Scheuchl, B., Schrama, E.J.O., Smith, B., Sundal, A.V., van Angelen, J.H., van de Berg, W.J., van den Broeke, M.R., Vaughan, D.G., Velicogna, I., Wahr, J., Whitehouse, P.L., Wingham, D.J., Yi, D., Young, D., Zwally, H.J., 2012. A reconciled estimate of ice-sheet mass balance. Science 338, 1183–1189.
Stoker, M.S., Stewart, F.S., Paul, M.A., Long, D., 1992. Problems associated with seismic facies analysis of Quaternary sediments on the northern UK continental margin. Soc. Underw. Technol. 28, 239–262.
Stroeven, P.A., Stroeven, P., van der Meer, J.J.M., 2005. Microfabric analysis by manual and automated stereological procedures: a methodological approach to Antarctic tillite. Sedimentology 52, 219–233.
Thomason, J.F., Iverson, N.R., 2006. Microfabric and microshear evolution in deformed till. Quatern. Sci. Rev. 25, 1027–1038.
van der Meer, J.J.M., 1993. Microscopic evidence of subglacial deformation. Quatern. Sci. Rev. 12, 553–587.
van der Meer, J.J.M., 2000. Microscopic observations on the first 300 metres of CRP-2/2A, Victoria Land Basin, Antarctica. Terra Antarct. 7, 39–348.
van der Meer, J.J.M., Hiemstra, J.F., 1998. Micromorphology of Miocene diamicts, indications of grounded ice. Terra Antarct. 5, 363–366.
van der Meer, J.J.M., Menzies, J., 2011. The micromorphology of unconsolidated sediments. Sediment. Geol. 238, 213–232.
van der Veen, C.J., Jezek, K.C., Stearns, L., 2007. Shear measurements across the northern margin of Whillans Ice Stream. J. Glaciol. 53, 17–29.
Vaughan-Hirsch, D.P., Phillips, E., Lee, J.R., Hart, J.K., 2012. Micromorphological analysis of poly-phase deformation associated with the transport and emplacement of glaciotectonic rafts at West Runton, north Norfolk, UK. Boreas 42, 376–394.
Watling, L., 1988. Small-scale features of marine sediments and their importance to the study of deposit-feeding. Mar. Ecol. 41, 135–144.
Whillans, I.M., van der Veen, C.J., 2001. Transmission of stress between an ice stream and interstream ridge. J. Glaciol. 47, 433–440.
Whillans, I.M., Bentley, C.R., van der Veen, C.J., 2001. Ice streams B and C. In: Alley, R.B., Bindschadler, R.A. (Eds.), The West Antarctic Ice Sheet: Behavior and Environment. American Geophysical Union, Antarctic Research Series 77, Washington, DC, pp. 257–281.

Williams, T., van de Flierdt, T., Hemming, S.R., Chung, E., Roy, M., Goldstein, S.L., 2010. Evidence for iceberg armadas from East Antarctica in the Southern Ocean during the late Miocene and early Pliocene. Earth Planet. Sci. Lett. 290, 351–361.

Whitehead, J.M., Bohaty, S.M., 2003. Pliocene summer sea surface temperature reconstruction using silicoflagellates from Southern Ocean ODP Site 1165. Paleoceanography 18. http://dx.doi.org/10.1029/2002PA000829.

Whitehead, J.M., Wotherspoon, S., Bohaty, S.M., 2005. Minimal Antarctic sea ice during the Pliocene. Geology 33, 137–140.

Winter, D., Iwai, M., 2002. Data report: Neogene diatom biostratigraphy. In: Barker, P.F., Camerlenghi, A., et al. (Eds.), Antarctic Peninsula Pacific Margin, ODP Leg 178 Rise Sites. Ocean Drilling Program, College Station, TX, pp. 1–25.